Journal of Medicinal Chemistry

Article

Discovery of highly potent and selective small-molecule reversible Factor D inhibitors demonstrating alternative complement pathway inhibition in vivo

Edwige Lorthiois, Karen Anderson, Anna Vulpetti, Olivier Rogel, Frederic Cumin, Nils Ostermann, Stefan Steinbacher, Aengus Mac Sweeney, Omar Delgado, Sha-Mei Liao, Stefan Randl, Simon Rüdisser, Solene Dussauge, Kamal Fettis, Laurence Kieffer, Andrea de Ekernez, Louis Yang, Constanze Hartwieg, Upendra A Argikar, Laura R. LaBonte, Ronald Newton, Viral Kansara, Stefanie Flohr, Ulrich Hommel, Bruce Jaffee, and Jürgen Maibaum

J. Med. Chem., **Just Accepted Manuscript** • Publication Date (Web): 16 Jun 2017

ACS Publications

Journal of Medicinal Chemistry is published by the American Chemical Society. 1155 Sixteenth Street N.W., Washington, DC 20036

Discovery of highly potent and selective small-molecule reversible Factor D inhibitors demonstrating alternative complement pathway inhibition *in vivo*

Edwige Lorthiois,[a*] Karen Anderson,[b] Anna Vulpetti,[a] Olivier Rogel,[a] Frederic Cumin,[a] Nils Ostermann,[a] Stefan Steinbacher,[c] Aengus Mac Sweeney,[a††] Omar Delgado,[b] Sha-Mei Liao,[b] Stefan Randl,[a†] Simon Rüdisser,[a] Solene Dussauge,[a] Kamal Fettis,[a] Laurence Kieffer,[a] Andrea de Erkenez,[b] Louis Yang,[b] Constanze Hartwieg,[a] Upendra A. Argikar,[b] Laura R. La Bonte,[b] Ronald Newton,[b] Viral Kansara,[b] Stefanie Flohr,[a] Ulrich Hommel,[a] Bruce Jaffee,[b] Jürgen Maibaum[a*]

[a] Novartis Pharma AG, Novartis Institutes for BioMedical Research, Novartis Campus, CH-4056 Basel, Switzerland, [b] Novartis Pharma AG, Novartis Institutes for BioMedical Research, Cambridge, Massachusetts 02139, USA, [c] Proteros Biostructures GmbH, D-82152 Planegg-Martinsried, Germany

KEYWORDS: Alternative Complement Pathway, Factor D inhibitors, S1 serine protease, structure-based drug design, MAC deposition, age-related macular degeneration.

ABSTRACT: The highly specific S1 serine protease Factor D (FD) plays a central role in the amplification of the complement alternative pathway (AP) of the innate immune system. Genetic associations in humans have implicated AP activation in age-related macular degeneration (AMD), and AP dysfunction predisposes individuals to disorders such as paroxysmal nocturnal hemoglobinuria (PNH) and atypical hemolytic uremic syndrome (aHUS). The combination of structure-based hit identification and subsequent optimization of the center (*S*)-proline-based lead **7** has led to the discovery of non-covalent reversible and selective human Factor D (FD) inhibitors with drug-like properties. The orally bioavailable compound **2** exerted excellent potency in 50% human whole blood *in vitro* and blocked AP activity *ex vivo* after oral administration to monkeys as demonstrated by inhibition of membrane attack complex (MAC) formation. Inhibitor **2** demonstrated sustained oral and ocular efficacy in a model of lipopolysaccharide (LPS)-induced systemic AP activation in mice expressing human FD.

Introduction

The alternative pathway (AP) of the complement system, when triggered by pathogen- or damage-associated molecular patterns on non-host and injured host cells, provides an innate immune defense mechanism in all vertebrates.[1,2] The AP also functions as an amplification mechanism for both the classical and the lectin pathways. A low level of steady complement activation by AP "tick-over" results in the generation of a small fraction of soluble C3-convertase in plasma (Figure 1). Upon activation, the initial C3-convertase cleaves complement C3 into the anaphylatoxin C3a and the larger fragment C3b, which binds to cell surfaces (opsonization) and recruits Factor B (FB), a pro-enzyme of the S1 serine protease family. FD cleaves FB in its complex with C3b thereby generating the active surface-bound C3-convertase

(C3bBb). C3bBb stabilized by properdin (P) cleaves additional molecules of C3, thus triggering a local amplification of AP activation, and moreover by recruitment of additional C3b generates the C5-convertase (C3bC3bBb). C3- and C5-convertases are key players in the alternative complement pathway ultimately leading to the formation of the membrane attack complex (MAC) and cell lysis. Dysregulation of AP and activation against the host has been connected to a variety of diseases such as age-related macular degeneration (AMD), atypical hemolytic uremic syndrome (aHUS), membranoproliferative glomerulonephritis type II (MPGNII) and paroxysmal nocturnal hemoglobinuria (PNH).[1,3] The S1 protease FD plays a central function in AP amplification by catalyzing the first and rate-limiting proteolytic step. FD is highly substrate specific due to a unique active site architecture that requires an induced-fit conformational transition to acquire full proteolytic activity. The extremely high specificity of FD is essential as it circulates in the blood as a mature enzyme, albeit adopting a latent active site conformation, and is not regulated by any known endogenous inhibitor.[4-6]

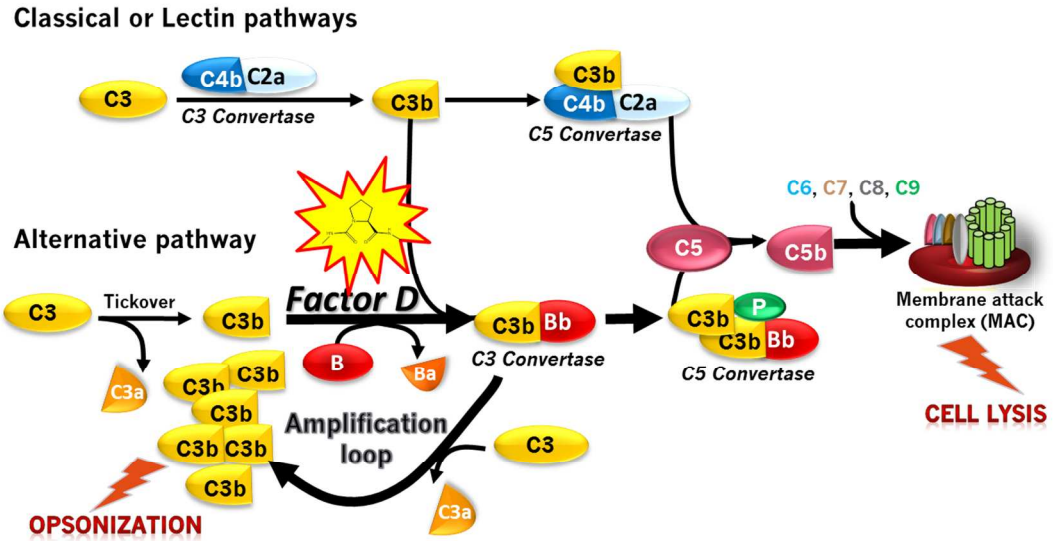

Figure 1: Schematic drawing of the classical, the lectin and the alternative complement pathways, highlighting the pivotal role of the S1 serine protease Factor D. An inhibitor of Factor

D has the potential to block the initiating step of the alternative pathway (AP) and the amplification loop that augments the other two pathways, and prevent the formation of the AP C3 and C5 convertases. The key effector mechanisms of innate immunity contributed by complement are opsonization by C3 fragments and lysis by deposition of the membrane attack complex (MAC) on cell surfaces.

As a consequence, FD inhibition appears to be an attractive mechanism to block the complement AP with high specificity and efficiency. For this reason, we had embarked in 2006 on an extensive drug discovery effort in the quest to develop orally effective, reversible non-covalent FD inhibitors useful for clinical therapy.[7,8] When we initiated our project, the only reported FD inhibitors were non-selective and covalent-irreversible, such as 2-carbamimidoylbenzo[b]thiophen-6-yl thiophene-2-carboxylate (BCX-1470),[9] properties that were considered as incompatible with selective and sustained AP inhibition required for disease therapy, in particular in view of the short plasma half-life of FD.[4a] Furthermore, no small molecule AP inhibitor has become available to date for clinical use.[10,11] Our multiple parallel approaches for initial hit identification included structure-based S1 target family scaffold hopping and tailored library design, focused fragment-based screening (FBS), screening of diverse Novartis corporate fragment libraries and function-based high-throughput screening using assays for FD thioesterolysis and for AP-mediated MAC deposition. Subsequent merging of newly discovered structural motifs essential for binding to the unique conformation of the latent FD active site together with further structure activity relationship (SAR) optimization eventually culminated in the center (*S*)-proline-based FD inhibitors **1** and **2** (Chart 1).[7] These compounds were shown to efficiently block alternative pathway (AP) activation and to prevent lysis of PNH erythrocytes *in vitro*.[7] We describe herein a more detailed account of our work

leading to the novel inhibitor **2** with promising *in vitro* selectivity and safety profiles, distribution into ocular tissues and demonstrating *in vivo* and *ex vivo* efficacy after oral administration in animal models of complement activation. Small-molecule potent and selective FD inhibitors were very recently reported by researchers at Achilion, however, without disclosing the origin and chemical structure of these compounds. ACH-4471 which has entered into early clinical investigation was shown to block *ex vivo* induced AP activity in cynomolgus monkeys after oral dosing, to reduce complement-mediated hemolysis of PNH erythrocytes and to block dysregulated AP activity *in vitro* in aHUS patient serum.[12]

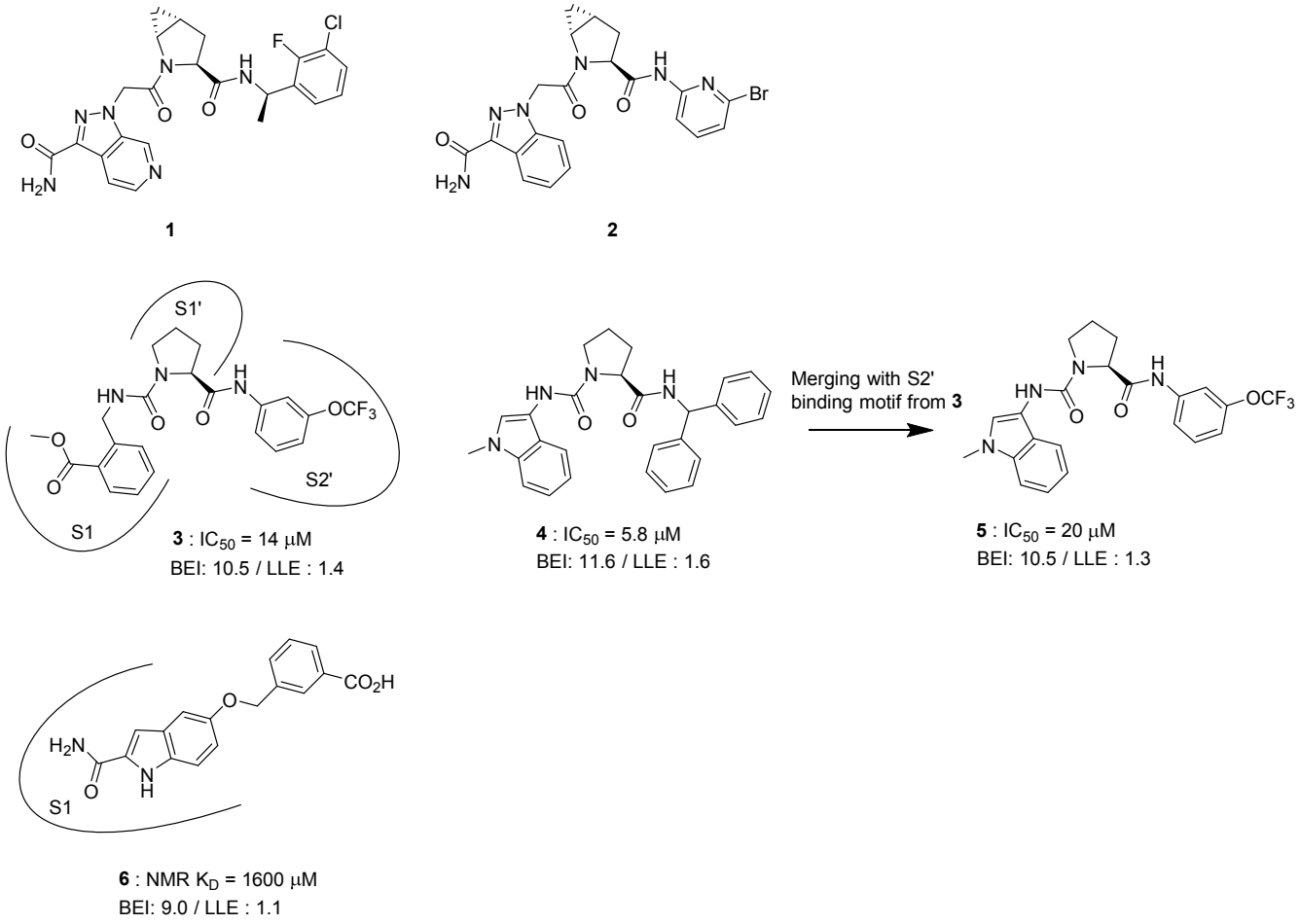

Chart 1.Chemical structures of compounds **1**–**6**.

Results and Discussion

As previously reported,[7,8] the center (*S*)-proline-based FD inhibitor **3** (Chart 1), was identified from a structure-based library design approach inspired by a structurally related analog binding to kallikrein 7, a member of the S1 protease family, and demonstrated moderate potency in blocking the thioesterolytic activity of latent human FD. Inhibitor **3** was shown by X-ray crystallography to bind in a bent conformation to the S1, S1' and S2' pockets of FD, in which the salt bridge between Asp_{182} and Arg_{218} at the bottom of the S1 pocket is present (closed conformation). Initial broad SAR exploration of the various portions of molecule **3**, in part by iterative small library design, failed to deliver any analogs with significantly improved *in vitro* potencies in the FD thioesterolysis assay (data not shown). Gratifyingly, the *N*-urea (*S*)-proline analog **4** (Chart 1) was uncovered by structure-similarity searches in the corporate compound collection and found to be a modest inhibitor of FD in the thioesterolysis assay. Computational modeling predicted the *N*-methyl-1*H*-indol-3-yl pharmacophore to bind into the S1 pocket.[7] However, the generation of an X-ray crystal structure of **4** in complex with recombinant human FD by both crystal soaking and co-crystallization remained unsuccessful in our hands, despite significant efforts. We therefore prepared its close analog **5**, in which the bulky diphenylmethane-amido residue is replaced by the less hydrophobic *meta*-OCF_3-anilide motif of **3** (Chart 1). Although compound **5** was ~4-fold less potent toward FD, as compared to **4**, the X-ray crystal structure of **5** bound to the active site of FD could be eventually resolved (Figure 2A). The electron density map was consistent with a single binding conformation of **5**, revealing the indole scaffold to be positioned in the S1 pocket and the *N*-methyl group pointing toward the side chain of Arg_{218} at the bottom of this binding site. The (*S*)-proline and the *meta*-OCF_3-anilide

portion of **5** occupied the S1'-S2' specificity pockets in a very similar manner as observed for the parent inhibitor **3** (PDB code: 5FBE).[7]

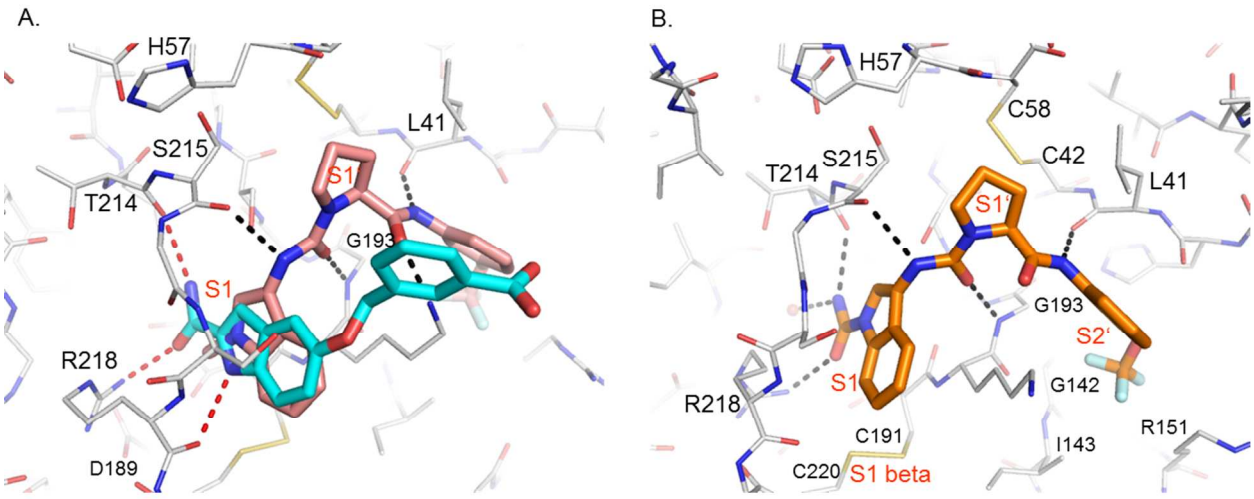

Figure 2. A. Crystal structure of the complex between human FD and **5** (in pink) (PDB code: 5NAT) overlaid with FD-bound **6** (in cyan) (PDB code: 5FBI). Hydrogen-bond interactions of the urea carbonyl to the Gly_{193} NH (oxyanion hole) and the amide NH of compound **5** to the backbone carbonyl of Leu_{41} are highlighted, as well as the H-bonds of the terminal carboxamide of **6** to Thr_{214} of the self-inhibitory loop and to Arg_{218} at the bottom of the S1 pocket, and the H-bond of the indole-NH with the Arg_{218} backbone carbonyl. Note that the benzoic acid portion of **6** is positioned in solvent space, and hence is not resolved in the crystal structure. **B**. Crystal structure of the complex between human FD and **7** (in orange) (PDB code: 5NAR). The imidazole side chain of the catalytic His_{57} is in an "out" conformation. The network of H-bonds between the *N*-carbamoyl residue of **7** and Thr_{214}, Arg_{218} and a water molecule bound deeply in the S1 pocket is highlighted.

The indole-carboxamide fragment **6** (Chart 1), which had previously been identified through screening of a focused set of fragments, was shown by ^{1}H-^{15}N HSQC-NMR to bind with very weak affinity to FD, and by X-ray crystallography to be accommodated by the S1 pocket of latent FD in its closed conformation.[7,8] Remarkably, the indole moiety of both **6** and **4** adopted a very similar planar orientation within the S1 pocket and sandwiched between the Lys_{192} side chain on one side and the self-inhibitory loop on the other side (Figure 2A). Moreover, the closely overlapping positions of the indole nitrogen atom of **4** and the C2 atom of **6**, as well as the respective bond vectors, suggested combining these structural motifs (Figure 2). As a consequence, compound **7** bearing an *N*-carbamoyl substituted indole was synthesized and demonstrated a remarkable 40-fold increase in inhibitory activity in the FD thioesterolysis assay, as compared to **5** (Table 1). The Binding Efficiency Index (BEI)[13-16] and the Lipophilic Ligand Efficiency (LLE)[17-20] for **7** (BEI: 13.3; LLE: 3.54) were improved compared to that calculated for compounds **3**–**6** (Chart 1). Importantly, compound **7** revealed similar potency with an IC_{50} value of 0.8 μM in the FD proteolysis assay using human FB in complex with cobra venom factor (CVF:FB), which is an ortholog of the activated human C3, as the endogenous surrogate substrate.[7] The (2*R*)-configured enantiomer **8** was 60-fold less active in the FD thioesterolytic assay (Table 1). The X-ray crystal complex of **7** bound to FD (Figure 2B) was determined at 1.55 Å resolution using the soaking method. The *N*-carbamoyl group of **7**, being key for strong binding affinity, is positioned deeply in the S1 pocket, as expected, and is engaged in direct H-bond interactions with the terminal guanidine nitrogen of the Arg_{218} side chain and the backbone carbonyl of Thr_{214} in a similar manner as was previously observed in the crystal structure of fragment **6** bound to FD (Figure 2A). In addition, one of the amide NH is in H-bond distance to an enzyme-bound water molecule positioned in a polar environment comprising the Ile_{227} amide

backbone and the hydroxyl of the Thr_{214} side chain. An additional interaction between the NH of the urea S1-S1' spacer in **7** and the Ser_{215} backbone carbonyl is also observed. The corresponding (*S*)-proline scaffold and the OCF_3-anilide moiety of both **7** and **3** are closely superpositioned in the S1'-S2' prime sites (not shown).

Compound **7** showed excellent selectivity against a panel of 10 human S1 proteases including kallikrein 7, chymotrypsin, trypsin, coagulation factor Xa, thrombin, plasmakallikrein and neutrophil elastase (all IC_{50} values >30 μM), and furthermore against a standard safety panel of 26 enzymes, receptors, ion channels and transporters (IC_{50} values >30 μM; weak affinities for adenosine 3 receptor (Ad3: 8.8 μM), adenosine transporter (AdT: 4.2 μM) and cyclo-oxygenase 1 (COX-1: 6.4 μM)). Also, **7** did not inhibit the hERG channel (IC_{50} >30 μM; dofetilide binding assay) and showed no signs for *in vitro* genotoxicity (mini-AMES[21] and Micronucleus test[22]). No inhibition of the cytochrome P450 enzymes CYP3A4 and CYP2D6 (IC_{50} >30 μM) and only weak inhibitory activity against CYP2C9 (IC_{50} = 3.4 μM) was observed. Inhibitor **7** displayed modest solubility, medium permeability in the Caco-2 assay (Table 4) and moderate *in vitro* clearance in rat and human liver microsomes (not shown). Importantly, the compound displayed a promising *in vivo* pharmacokinetic profile in Sprague-Dawley (SD) rats (dosed at 1 mg/kg intravenously (IV) and at 10 mg/kg orally (PO)), characterized by moderate clearance (CL = 21 mL/min/kg), a terminal half-life ($T_{1/2}$) of 1.4 h, sustained micromolar exposure levels in plasma ($AUC_{0\text{-}8\ h}$ = 4990 nMh; C_{max} = 1167 nM) and 25% oral bioavailability. Based on its overall properties, we considered compound **7** as a reasonable starting point for further SAR exploration. Our initial efforts were aimed at optimizing the binding interactions to the S1, S1' and S2' pockets considered as hot spots in the active site of latent FD,[8] rather than expanding into the S1β region, with the objective to improve potency not at the expense of BEI[13-16] and LLE.[17-20]

We reasoned that additional contacts to the S1' site, in particular to the small indentation defined by the His_{57} backbone, the Cys_{42}-Cys_{58} disulfide bridge and the Ser_{215} side chain (Figure 2), would improve FD binding. Accordingly, alterations of the (*S*)-proline scaffold were envisaged by introducing small hydrophobic substituents to C4 and/or C5 of the center ring with appropriate absolute configuration (Table 1). Introduction of a methyl group to the 4-position of the proline, either with absolute (*R*)- or (*S*)-configuration (compounds **9** and **10**, respectively), and likewise the incorporation of a fused *trans*-3,4-cyclopropyl-proline (**11**), did not significantly influence the *in vitro* potency, as compared to **7**, when tested in the biochemical FD assay. Replacing the pyrrolidine by a piperidine center ring resulted in a dramatic loss in potency (**12**). In contrast, and very gratifyingly, attaching a fused *trans*-4,5-cyclopropyl ring to the proline scaffold gave a 10-fold improvement in potency with **13** displaying an IC_{50} value of 50 nM. The potency of **13** was retained when measured in the CVF:FB proteolytic ELISA assay (IC_{50} = 0.21 μM), and moreover **13** inhibited AP activation *in vitro* in a functional membrane attack complex (MAC) deposition assay using 50% human whole blood,[7] albeit with a 20-fold decrease in activity (Table 2).

To inform further medicinal chemistry design, we determined the crystal structure of **13** in complex with FD (Figure 3A). The overall binding pose of **13** emulating the U-shaped active site conformation of latent FD extending from S1 to S2' was confirmed, with the His_{57} again adopting a 'non-canonical' catalytic-triad conformation. The (*S*)-proline ring portion of the bicyclic aza-bicyclo[3.1.0]hexane scaffold adopted a very similar bound conformation as observed for the unsubstituted analog **7** (Figure 3A). The axial methylene group of the cyclopropyl ring is oriented toward the back-surface of the S1' site and forms close van der

Waals contacts by nicely filling the small hydrophobic indentation which is formed as a consequence of the flipped conformation of the His_{57} side chain.

Table 1. *In vitro* Potency Data for Compounds **7**–**18**, using a FD Thioesterolytic Fluorescent Assay.

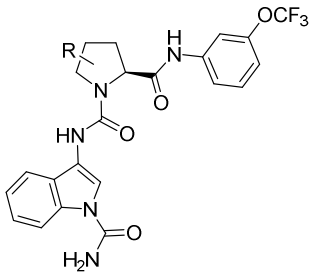

Entry	Cpd	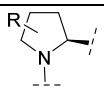	FD IC_{50} (μM)[a,b]
1	**7**		0.50
2	**8**	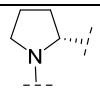	30
3	**9**	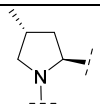	0.85
4	**10**	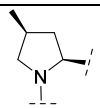	0.30
5	**11**	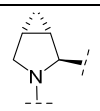	0.65
6	**12**	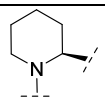	22
7	**13**	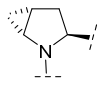	0.05
8	**14**	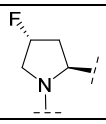	0.05

9	**15**	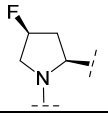	0.70
10	**16**	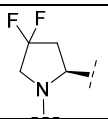	0.45
11	**17**	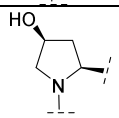	1.4
12	**18**	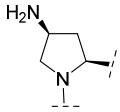	0.50

[a]Half–maximal inhibition of recombinant human complement FD catalytic domain, as determined in a thioesterolysis-based assay using Z-Lys-thiobenzylester as the substrate. [b]Data represent mean values of duplicate measurements.

To explore the impact of the C4-substitution and stereochemistry by introducing a fluorine atom to the center pyrrolidine, the (*R*)- and (*S*)-configured mono-fluoro analogs **14** and **15**, as well as the 4,4-difluoro derivative **16**, were synthesized. A 10-fold improvement in potency was accomplished for (4*R*)-**14**, whereas both the (4*S*)-diastereomer **15** and the difluoro analog **16** were found to be equipotent to the parent compound **7** (Table 1). The stereo-dependent effects of a fluorine and other heteroatoms substituting the C3 and C4 positions of N-acylated proline-carboxamides on ring puckering is well documented.[23] A fluorine at position C4 of the proline alters the relative energies of the ring puckers, which can lead to the nearly exclusive population of a single conformer. The C_4-*endo* conformation is preferred for 4(*S*)-fluoro-proline mono-substituted derivatives, whereas 4(*R*)-fluoro-prolines adopt the C_4-*exo* conformation which in case of (4*R*)-**14** is expected to direct the fluorine atom toward the S1' back-surface, thereby enhancing the van der Waals interactions to the protein. Moreover, the presence of the (4*R*)-fluorine results in a preference for the *trans*-peptidic bond of the *N*-acyl proline resembling the

FD bound conformation observed for inhibitors **7** and **13**.[23] The X-ray crystal structure of **14** bound to FD (Figure 3A) indeed revealed the proline ring in a C_4-*exo* pucker, thereby positioning the F-atom close to the Cys_{48}-Cys_{52} disulfide bridge and the His_{57} backbone carbonyl. The anti-parallel dipole-dipole interaction observed between the large C-F dipole and the His_{57} carbonyl dipole may further contribute to the improved binding affinity of **14** (Figure 3B). *Vice versa*, the fluorine of (4*S*)-**15** in its anticipated C_4-*endo* conformation is directed toward solvent space without being involved in direct binding interactions.

Next, we introduced polar substituents to C4 of the proline ring with the aim to improve aqueous solubility while retaining *in vitro* potency. Proline-amides bearing a (4*S*)-hydroxy or (4*S*)-amino group have been shown to preferentially adopt a C_4-*endo* ring pucker,[23] in line with our design concept to place a solubilizing group close to solvent space. Compound **17** bearing a (4*S*)-OH showed a ~3-fold drop in biochemical potency, whereas the more soluble (4*S*)-NH_2 analog **18** exhibited similar affinity for FD compared to **7**, despite the slightly reduced van der Waals contacts of the proline *endo*-pucker to the S1' hydrophobic surface observed in the FD/**18**-complex X-ray structure (depicted in Figure 3A).

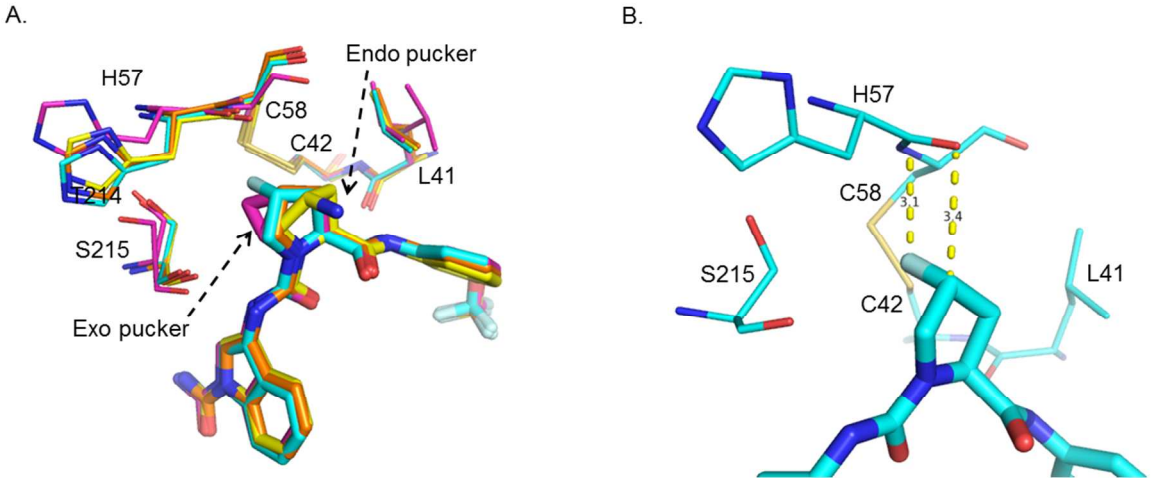

Figure 3.A. Superpositions of compounds **7** (in orange color), **13** (magenta) (PDB code: 5NAW), **14** (cyan) (PDB code: 5NBA) and **18** (yellow) (PDB code: 5NB6) observed in their X-ray crystal structures in complex to human FD. The conformational flexibility of the His_{57} and Ser_{215} side chains are highlighted, while the Cys_{42}-Cys_{58} disulfide bridge conformation is largely conserved. **B**. Close-up view highlighting the anti-parallel dipole-dipole interaction observed between the C-F dipole in **14** and the FD His_{57} carbonyl dipole.

We next focused our efforts on exploring the S2' region identified as hydrophobic hotspot defined by Gly_{142} and the side chains of Ile_{143} and Arg_{151}.[8] The trifluoromethoxy-phenyl residue in its energetically favoured perpendicular conformation[24-26] positions the highly lipophilic CF_3 moiety deeply into the S2' pocket, thereby tightly filling the small hydrophobic indentation of the enzyme (Figure 4A). Replacement of the OCF_3 group in **13** by a $OCHF_2$ (**19**) decreased potency by 3-fold, whereas the OCH_3 analog **20** showed a more pronounced 6-fold potency drop likely due to the favoured in-plane conformation of the methoxy-anilide portion[24-26] (Table 2). Halogen replacements were tolerated with a preference for bromine over a chlorine atom (**22** *vs*. **21**), reflecting the increase in strength of the halogen bond to the backbone carbonyl of Trp_{141} as a result of the increase in halogen size (*vide infra* for a more detailed discussion).[27-30]

Table 2. *In vitro* Potency Data for Compounds **13, 19–26**, using a FD Thioesterolytic Fluorescent Assay and a MAC Deposition Assay.

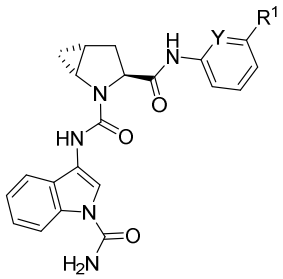

Entry	Cpd	Y	R^1	FD IC_{50} (μM)[a,c]	MAC IC_{50} (μM)[b,c]	hPPB (%)[e]
1	**13**	CH	OCF_3	0.05	1.25	nd
2	**19**	CH	$OCHF_2$	0.15	nd[d]	nd
3	**20**	CH	OCH_3	0.32	nd	nd
4	**21**	CH	Cl	0.15	nd	nd
5	**22**	CH	Br	0.045	nd	nd
6	**23**	CF	OCF_3	0.012	0.250	nd
7	**24**	CF	CF_3	0.023	0.587	>99
8	**25**	N	CF_3	0.014	0.022	95.2
9	**26**	N	Br	0.006	0.009	96.4

[a]Half–maximal inhibition of recombinant human complement FD catalytic domain, as determined in a thioesterolysis-based assay using Z-Lys-thiobenzylester as the substrate; [b]Half–maximal inhibition of soluble MAC complex formation, as determined in an ELISA assay using alkaline-phosphatase-conjugated-anti-C9-neoepitope in normal human whole blood diluted with

an equal amount of gelatine veronal buffer; [c]Data represent mean values of duplicate measurements; [d]Not determined; [e]Compound fraction in % bound to human plasma protein.

The concept of introducing an additional fluorine atom at the 2-position of the P2' anilide moiety of **13** derived from SAR data for structurally related proline-based FD inhibitors, such as **1**, bearing *ortho*-F substituted benzylamides at P2'.[7] Compound **23** was found to be 4-times more potent than the des-fluoro analog **13** in both the thioesterolysis assay and in the MAC deposition assay (Table 2). The gain in potency could be explained by the conformational preference of the anilide moiety induced by the presence of the *ortho*-F adjacent to the amidocarbonyl spacer, properly directing the *meta*-OCF_3 into the S2'pocket.[23,31] The conformation with the fluorine *cis* to the amide carbonyl is destabilized by electrostatic repulsion, while the preferred *trans* conformation is favoured by the formation of the NH/CF 1,3-antiperiplanar dipolar interaction. In addition, the improvement in potency observed upon introduction of the *ortho*-F might also be the result of the increased aniline N-H acidity, thereby strengthening the H-bond with the Leu_{41} backbone carbonyl.

Replacement of the 2-fluoro-aniline by a 2-aminopyridine residue was designed to have a similar effect on the ligand conformation due to a repulsion between the nitrogen atom of the pyridine and the carbonyl of the amide P1'-P2' linker. Compounds **24** bearing a 2-F,3-CF_3-aniline P2' motif and **25** bearing a 6-CF_3-pyridine were found to be equipotent in the biochemical assay (Table 2). Notably, in the MAC deposition assay performed using 50% human whole blood, a lower 'IC_{50} shift' was observed for **25** compared to **24**, which could be attributed to the lower % fraction of compound **25** bound to human plasma protein (hPPB) as compared to **24** (Table 2). Most strikingly, the 6-bromo-pyridine analog **26** exhibited single-digit nanomolar potency in

both assays in line with the moderate hPPB of **26** and consistent with our more general observation that pyridyl P2'-residues resulted in reduced 'IC_{50} shifts' between the biochemical and MAC deposition assays. We reasoned that the pyridyl nitrogen further increases the size of the σ-hole of the bromine atom[29,32] leading to an increase in the strength of the halogen bond with the carbonyl of Trp_{141} (*vide infra*).

With the attractive P1' cyclopropyl proline and the 2-amino-6-bromo-pyridine S2'-binding motif in hand, we next turned our attention to the optimization of the P1 indole carboxamide portion. The contact between the NH of the urea P1-P1' spacer in **7** and the Ser_{215} backbone carbonyl in the crystal structure complex with FD (Figure 2B) was recognized to be sub-optimal. In addition, the dihedral angle between the indole plane and that of the urea group has to be almost perpendicular in order to allow for the accommodation of the indole scaffold in the S1 pocket. As such a conformation is likely less favoured energetically in solution, we sought to properly modify the spacer. Compound **27** harboring a potentially more beneficial amide spacer, however, was found to be 30-fold less potent than **23** (Table 3). In contrast, the inverted-indole analog **28** demonstrated improved potency with only a 10-fold loss compared to **26** in the biochemical assay. In the case of **28**, the slightly more acidic protons of the amide linker may weakly contribute to a favorable contact with the Ser_{215} backbone carbonyl. Surprisingly, a dramatic loss in potency was observed in the MAC deposition assay for **28**. In this case, % hPPB would not entirely explain the larger 'IC_{50} shift' observed for **28** as compared to compound **26** with slightly lower %PPB (Table 3). Most gratifyingly, a 10-fold boost in potency in both the biochemical and the MAC deposition assays was observed when the indole in **28** was replaced by an indazole moiety leading to compound **2** which is equipotent to **26** in the thioesterolysis assay and 5-fold less potent in the MAC deposition assay despite similar % hPPB. Notably, replacing the *N*-

carbamoyl group (**2**) by an *N*-acetyl group (**29**) had only a marginal impact on potency, which was unexpected in view of the observed H-bonding interactions between both hydrogen atoms of the terminal NH_2 deep in the S1 pocket[33] (Figures 2B, 4A), but which could possibly result from differences in desolvatation energies.

Table 3. *In vitro* Potency Data for Compounds **2, 23, 26**–**30**, using a FD Thioesterolytic Fluorescent Assay and a MAC deposition assay.

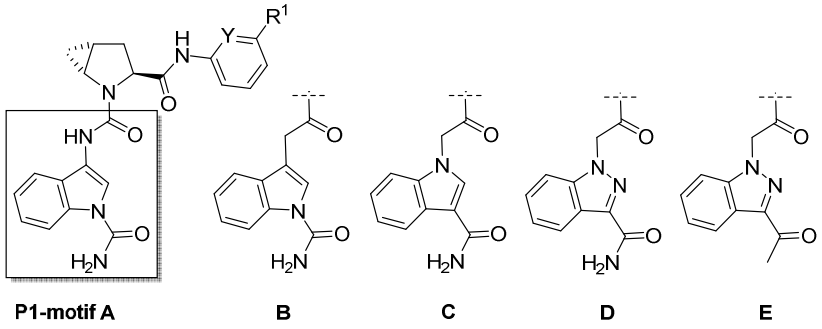

Entry	Cpd	Y	R^1	P1-motif	FD IC_{50} (μM)[a,c]	MAC IC_{50} (μM)[b,c]	hPPB (%)[e]
1	**23**	CF	OCF_3	A	0.012	0.25	nd
2	**27**	CF	OCF_3	B	0.37	nd[d]	nd
3	**26**	N	Br	A	0.006	0.009	96.4
4	**28**	N	Br	C	0.066	1.86	86.9
5	**2**	N	Br	D	0.006	0.05	92
7	**29**	N	Br	E	0.015	0.035	nd

6	**30**	CF	Br	D	0.010	0.15	nd

[a-e]For details, see Table 2.

We determined the X-ray crystal structure of **2** in complex with FD at high 1.33 Å resolution (Figure 4).[34] The overall binding mode of the proline scaffold and the indazole moiety to the S1 and S1' pockets, respectively, is very similar to the binding mode observed for **13.** The network of H-bonds in the S1 pocket and the H-bond between the amide spacer and the Leu_{41} backbone carbonyl are conserved for **2**. In contrast, the S2' binding modes are strikingly distinct for the two compounds with the 6-Br-pyridine motif (**27**) located in the lower part of the pocket, thereby positioning the bromine atom into the region that is occupied by the CF_3 moiety of the trifluoromethoxy-phenyl residue present in **13** (Figure 4B). Notably, the bromine atom forms a σ-hole halogen bond interaction with the backbone carbonyl of Trp_{141}.[27-30,33] The C_{pyr}-Br…O angle is 164.6º, thus fulfilling the typical angular preference with a measured bromine-oxygen distance (3.09 Å) significantly lower than the sum of the van der Waals radii (R_{vdW}Br-O: 3.37Å).[27,29] The pyridyl nitrogen in **2** further increases the size of the σ-hole of the bromine atom, thereby leading to an increase in the strength of the halogen bond with the carbonyl of Trp_{141}.[29] Similarly, the presence of an *ortho*-F atom in the 3-Br-anilide P2' moiety, as in **30**, is expected to strengthen the halogen σ-hole interaction[29,32] with the Trp_{141} carbonyl (Table 3).

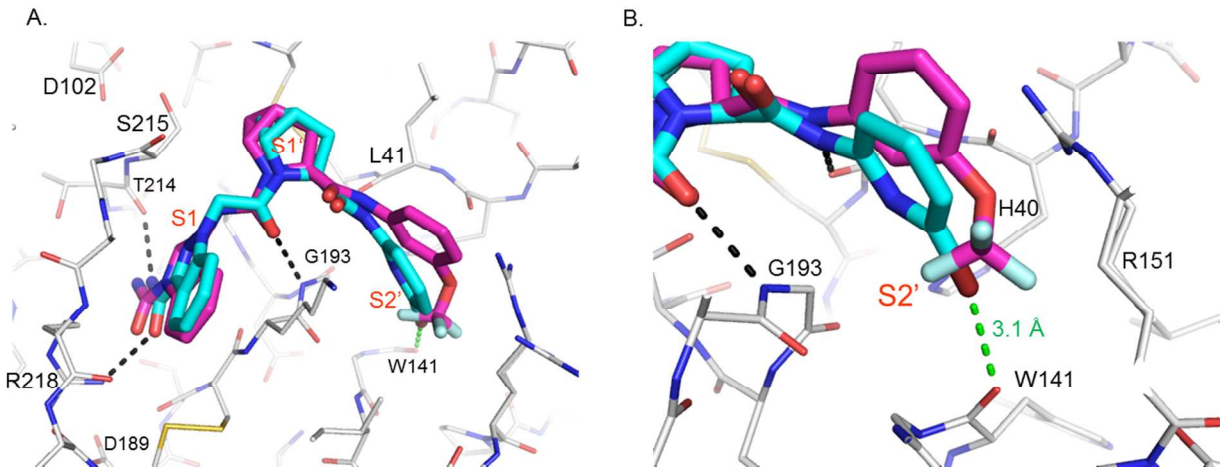

Figure 4. A. Crystal structures of human FD in complex with **2** (the protein is shown in grey color and the ligand in cyan color) (PDB code: 5NB7) overlaid with the crystal structure of the complex with compound **13** (only the ligand is shown, magenta color). The network of H-bonds (black dashed lines) in the S1 pocket, to the backbone of Gly_{193} and the H-bond between the amide spacer and Leu_{41} backbone carbonyl are conserved. **B**. Close up view of the S2' region, the halogen bond (green dashed lines) between the bromine atom in compound **2** and the Trp_{141} backbone carbonyl is highlighted.

To this point of our work, we had been quite successful in improving the *in vitro* potency by >2,000-fold, starting from our initial hit **3** and by iteratively optimizing the interactions of the inhibitors to each single key hot spot of the FD S1–S1'–S2' pockets, without any significant increase in ligand molecular size. This accomplishment is reflected in a remarkable increase in the BEI and LLE, respectively, for **2** (MW: 482; BEI: 17.1; LLE: 6.9, cLogP: 1.3), one of the most potent FD inhibitors discovered in this series, as compared to **3** (MW: 465; BEI: 10.4; LLE: 1.4; cLogP: 3.5). The ability to effectively manage MW and cLogP proved to be very important as increase in those parameters has been associated with deterioration of the ADMET profile.[35]

The initial lead compound **7** was shown to have modest aqueous solubility, moderate Caco-2 cell permeability, low-micromolar CYP2C9 inhibitory activity (Table 4). The presence of a fused 4,5-cyclopropyl ring (**13**), while slightly improving solubility, appeared to further increase CYP2C9 inhibition. Introduction of a polar OH or NH_2 substituent to the proline ring ameliorated CYP2C9 affinity (**17** and **18**), and in case of **18** improved solubility, albeit at the cost of permeability. Notably, both **14** and **17** demonstrated strong efflux in the Caco-2 permeability assay.

Table 4. High Throughput Equilibrium Solubility, Permeability and CYP2C9 Inhibition for (*S*)-Proline-based FD Inhibitors

Cpd	HT-eq solubility, pH 6.8 (mM)[a]	Caco-2 P_{app}(AB) /(BA)x 10^{-6}(cm/s) / ratio(BA)/(AB)	CYP2C9 IC_{50} (μM)[b]
7	0.017	6.1/ 6.3/ 1	3.4
13	0.077	4.5 / 5.7 / 1.3	0.8
14	0.007	0.75 / 8.0 / 10	2.5
17	0.023	0.77 / 17 / 22	>10
18	0.28	2.1 / 5.1 / 2.5	>10
23	0.01	5.1 / 6.5 / 1.3	0.25
24	0.046	10 / 7.0 / 0.7	0.15
25	0.11	11.3 / 14.2 / 1.3	4.3
26	0.057	9.6 / 10.3 / 1.1	4.0
2	0.17	15.3 / 18.1 / 1.2	>20

[a]Equilibrium high-throughput solubility in aqueous buffer (pH 6.8); [b]Diclofenac was used as CYP2C9 substrate.

Introduction of an *ortho*-F atom to the P2' aniline moiety, substituted by either OCF_3 or CF_3 (**23**, **24**), reduced solubility and led to sub-micromolar affinities for CYP2C9. In contrast, switching

from an aniline to a 2-aminopyridyl P2' motif led to a superior CYP2C9 profile by increasing the IC_{50} value ~30-fold for **25** and **26**, as compared to **24**, accompanied by a marginal improvement in solubility. Introduction of the 3-carboxamide indazole S1 motif (**2**) resulted in a slight improvement in aqueous solubility, cell permeability without efflux potential in Caco-2 cells and in the P450 inhibition profile (IC_{50} >20 and 17 μM for CYP2D6 and 3A4, respectively). The excellent overall selectivity of inhibitor **2** in a broad panel of proteases, kinases, receptors and ion-channels has been previously reported.[7] Furthermore, **2** did not inhibit the hERG channel (IC_{50} >30 μM; dofetilide binding and Qpatch assays) and showed no evidence for mutagenic, clastogenic or aneugenic potential when assessed in a miniaturized version of the Ames-test and in the standard *in vitro* micronucleus test, respectively.[21,22]

Chemistry

Efficient synthetic routes to access *N*-urea (compounds **5, 7**–**26**) and *N*-acylated (**2**, **27**–**30**) substituted proline-carboxamides are outlined in Scheme 1. Briefly, *N*-Boc protected (*S*)-, (*R*)-proline, as well as mono- and disubstituted proline analogs, all available as single stereoisomers from commercial sources, were coupled with substituted anilines or amino-pyridines, respectively, to afford the corresponding amide intermediates A. Removal of the *N*-Boc protecting group to intermediates B and subsequent reaction with 1-methyl-1*H*-indol-3-yl-isocyanate (**31**) or the 1-carbamoyl analog **32** furnished the *N*-urea linker derivatives **5**, **7**–**26**. Similarly, the HBTU-mediated coupling reaction of intermediates B with carboxylic acids **33**–**36** afforded target compounds **2**, **27**–**30** containing an amide linker. For the preparation of the 4(*S*)-amino-proline analog **18** from the commercially available (4*S*)-4-*N*-Fmoc-amino-1-Boc-L-

proline the deprotection of the Fmoc protecting group was performed using piperidine 20% in DMF (Scheme 1, step d).

Scheme 1. Synthetic Routes for Inhibitors 2, 5, 7 to 30[a] (*cf.* Tables 1–3 for Structures)

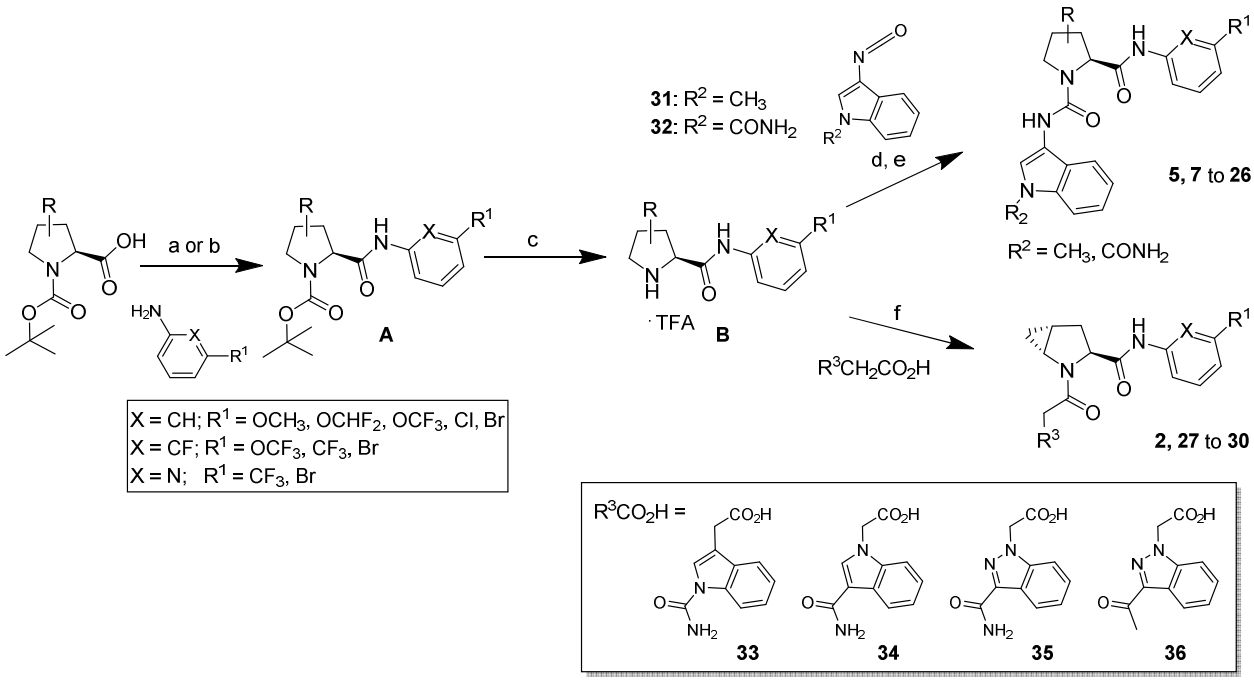

[a]Reagents and conditions: (a) HBTU, DIPEA, CH_2Cl_2 or DMF, RT or DMF, 70°C (for X = CF and $R^1 = OCF_3$); (b) 1-chloro-*N*,*N*,2-trimethylpropenylamine, CH_2Cl_2, 0°C (for X = N and R^1 = CF_3, Br); (c) TFA, CH_2Cl_2; (d) R^2NCO (**31** or **32**), Et_3N, THF; (e) piperidine 20% in DMF, RT for the Fmoc deprotection leading to **18**; (f) R^5CO_2H (**33**, **34**, **35** or **36**), HBTU, DIPEA, CH_2Cl_2, RT.

The 4(*R*)- and 4(*S*)-methyl-proline analogs **9** and **10** were prepared from the commercially available *N*-Boc-4-methylene-proline (**37**) by HBTU-coupling with 3-OCF_3-aniline to afford **38**, followed by hydrogenation reaction in the presence of Pd on charcoal to produce a mixture of diastereoisomers, which were separated by reversed-phase prep-HPLC to afford (2*S*,4*R*)-**39** and

(2*S*,4*S*)-**40**, respectively (Scheme 2). The absolute configuration was assigned based on ROESY-NMR experiments showing a nOe-effect between proton-H2 and the 4-methyl group for the *trans*-configured **39**, and on the other hand a nOe-effect between protons H2 and H4 for *cis*-**40**.

Scheme 2. Synthetic Routes for Intermediates 39/40[a]

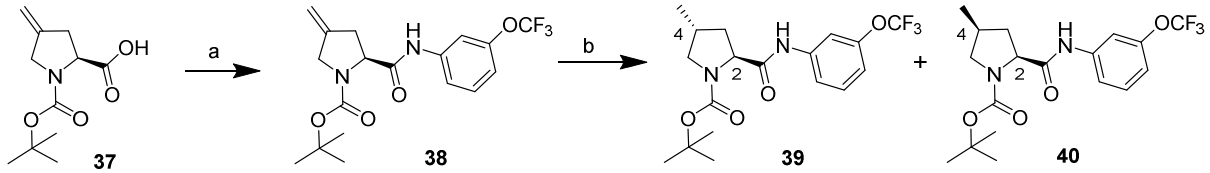

[a]Reagents and conditions: (a) HBTU, DIPEA, CH_2Cl_2, RT, 100%; (b) H_2, Pd/C, MeOH, **39** (7%) and **40** (53%).

Isocyanate **32** was prepared in four steps by starting from indole-3-carboxylic acid (**41**) by formation of benzylester **42**, *N*-carboxamidation using sodium hydride and chlorosulfonylisocyanate to produce **43**. This was followed by saponification to yield the carboxylic acid **45**, and finally by thermal Curtius rearrangement of the acyl azide intermediate formed from **45** in the presence of DPPA and Et_3N in toluene[36] (Scheme 3). It is important to note that the acyl azide intermediate prepared from acid **45** precipitates in the reaction mixture and must be purified by filtration before being added portion-wise[37] to hot toluene in order to ensure a smooth Curtius rearrangement. All attempts to perform this reaction in one pot from acid **45** failed to give the desired isocyanate **32**. The *N*-methyl indole isocyanate **31** was prepared accordingly from commercially available 1-methylindole-3-carboxylic acid (**44**) following a similar synthetic protocol.

Carboxylic acid **34** is commercially available and the synthesis of **35** (Scheme 1) has been reported previously.[7] The (1-carbamoyl-1*H*-indol-3-yl)-acetic acid (**33**) was prepared by *N*-carboxamidation of ethyl 2-(indol-3-yl)acetate (**46**) with chlorosulfonylisocyanate subsequent to deprotonation with NaH in THF followed by saponification, and acid **36** was obtained in two steps from 1-(1*H*-indazol-3-yl)ethan-1-one (**48**) by alkylation with *tert*-butylbromoacetate and final ester-deprotection under acidic conditions (Scheme 3).

Scheme 3. Synthetic Routes for Intermediates 31-33 and 36[a]

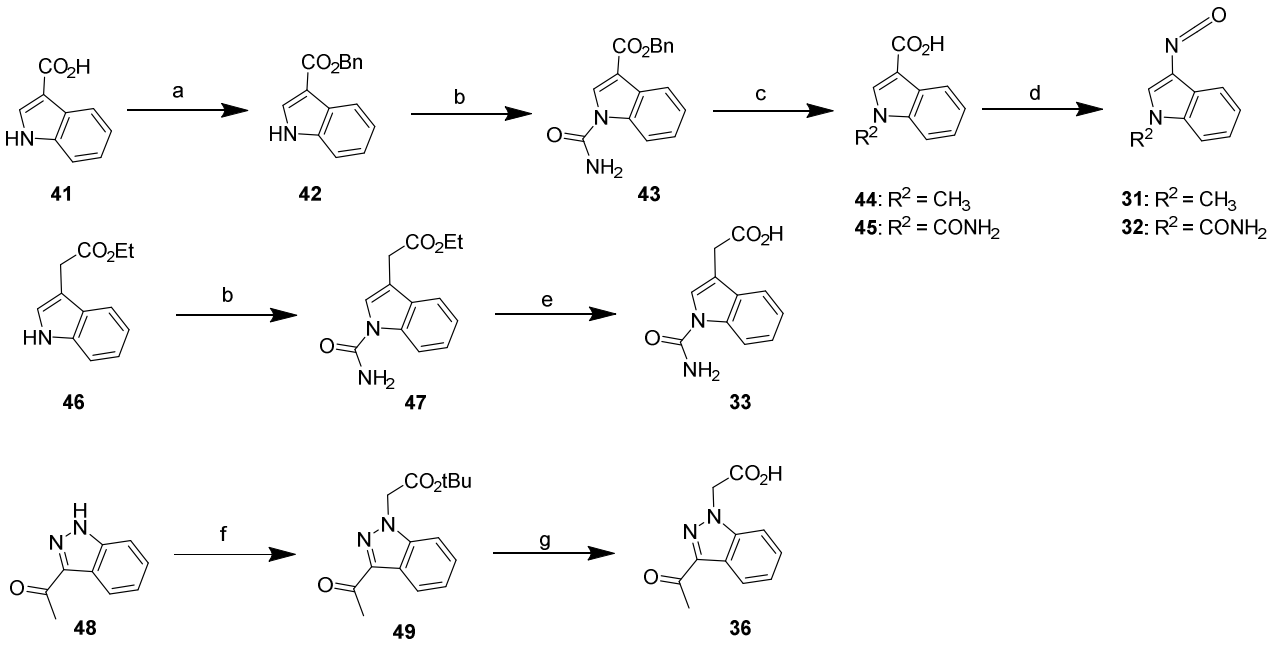

[a]Reagents and conditions:(a) BnBr, Cs_2CO_3, DMF (83%); (b) NaH, THF, $ClSO_2NCO$ (**43**: 29%; **47**: 75%); (c) H_2, Pd/C 10%, THF/ DMF, (100%); (d) (i) Et_3N, DPPA, CH_2Cl_2, -15 °C to 15 °C, (ii) toluene, reflux (**31**: 89%; **32**: 52%); (e) NaOH, MeOH/H_2O (95%); (f) $BrCH_2CO_2{}^tBu$, K_2CO_3, CH_3CN reflux; (g) TFA, CH_2Cl_2 (100% for 2 steps).

In vivo pharmacology

Since inhibitor **2** demonstrated an excellent *in vitro* profile, including high potency and selectivity, we further evaluated the potential of **2** for *in vivo* use, and for its ability to achieve exposure in the eye, given the evidence for the role of the AP in AMD.[38] Compound **2** displayed an excellent oral PK profile in Sprague Dawley rats,[7] and following an oral dose (10 mg/kg) in Brown Norway rats demonstrated a good distribution and sustained exposure in ocular tissues including the neural retina and the posterior eye cup (PEC), which comprises the sclera, retinal pigmented epithelium, and the choroid. Mean exposure levels in plasma, the PEC and the retina at 6 hours after dosing were 0.36, 0.43, and 0.09 µM, respectively (Figure 5). For context, these values exceeded significantly the IC_{50} for **2** in the *in vitro* MAC deposition assay (0.05 µM, Table 3).

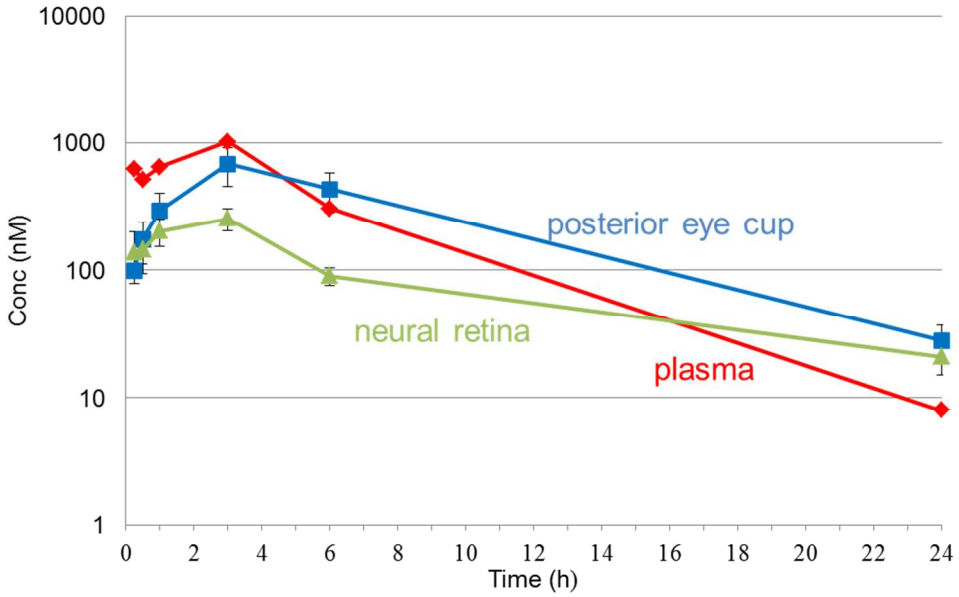

Figure 5. Plasma and ocular pharmacokinetics profiles of inhibitor **2** in Brown Norway rats after oral administration (10 mg/kg). The compound was formulated as a suspension in 0.5% HPMC and 0.1% Tween 80 and was administered by oral gavage to male 250 g Brown Norway rats (n = 2 per time point). Tissues from 2 animals were collected at 0.25, 0.5, 1, 3, 6 and 24

hours, respectively, for analysis (4 eyes/time point; each eye dissected into neural retina and posterior eye cup). Two plasma samples per time point were collected. Points represent the mean, and error bars represent the standard deviation.

In other studies we have shown that the significant difference in active site conformation of murine *vs.* human FD precludes the binding of our compounds.[7] To enable *in vivo* efficacy assessment, we generated mice that express only the human enzyme (human FD knock-in mice) at blood levels that are in the reported range for humans.[7] We developed a pharmacodynamic model of complement AP activation in these mice using lipopolysaccharide (LPS). Intraperitoneal administration of LPS induces activation of the AP, as detected by increased levels of AP breakdown products Ba and iC3b+C3d in the circulation and in the ocular tissues, respectively.[7] We administered **2** by oral gavage at 30 mg/kg to groups of human FD knock-in mice at different time points up to 24 hours prior to the end of the experiment. LPS was administered to all groups at 7.5 hours prior to the end of the experiment, so that all mice experienced the same window of complement activation. At study termination, plasma and eye tissue were collected for measurement of complement breakdown products. Compound **2** caused a sustained inhibition of Ba generation in the plasma, with suppression to or below baseline levels for up to 8 hours (Figure 6A). In the eye, complete suppression of complement activation was seen for at least 12 hours (Figure 6B).

A

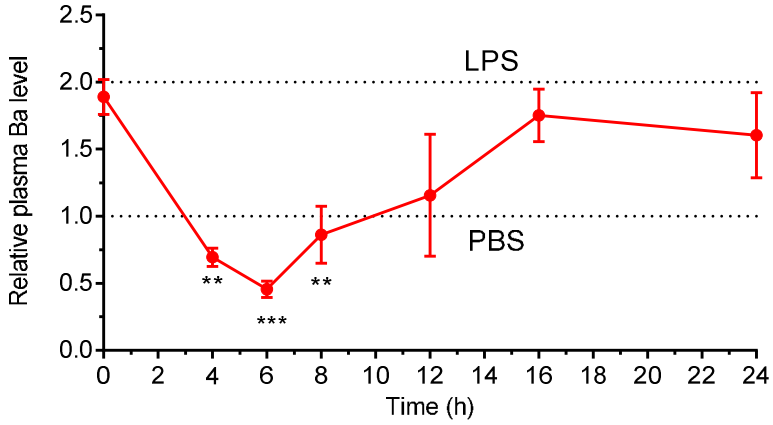

B

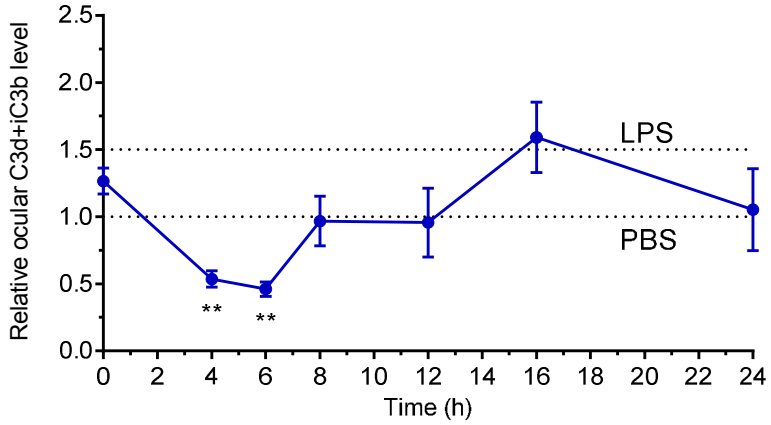

Figure 6. Inhibitor **2** tested at 30 mg/kg in the human factor D knock-in mouse pharmacodynamic model: (A) inhibition of Ba generation in plasma and (B) inhibition of iC3b and C3d generation in ocular tissues. Groups of mice (n = 4, female human FD knock-in) were treated either with **2** or dosing vehicle by oral gavage at 24, 16, 12, 8, 6, and 4 hours, respectively, prior to the termination of the study. All animals were given intraperitoneal LPS to activate complement 7.5 hours prior to study termination. Baseline complement levels were obtained from mice that received oral dosing vehicle and intraperitoneal saline (indicated by PBS line on graph). The positive control group received oral dosing vehicle and intraperitoneal LPS

(LPS line on graph). Data shown represent mean ± s.e.m. for the group. Statistical analysis was by ANOVA with Tukeys multiple comparison test, where ***P<0.001, **P<0.01 compared to the positive control group.

Inhibitor **2** was further investigated in cynomolgus monkeys to characterize the PK–PD relationship. *In vitro* potency of **2** was shown to be very similar against human and monkey FD (IC_{50} values in FD thioesterolytic assays of 0.005 μM and in 50% serum MAC deposition assays of 0.011 μM for both human and monkey). A pre-dose serum sample was collected from each animal to establish individual baseline complement activity. After a single oral dose of **2** at 10 or 50 mg/kg serum samples were obtained at 4, 7, and 24 hours post-administration. *Ex vivo* assessment for complement activity in serum was performed using zymosan to induce AP activation (Figure 7A). All monkeys showed complete suppression of complement activity in serum collected 4 hours after dosing. Individual blood levels of **2** were determined using liquid chromatography coupled to mass spectrometry (LC-MS). The *ex vivo* half-maximal efficacious concentration (EC_{50}) was determined to be 0.038 μM, with complete inhibition observed at exposures >0.5 μM (Figure 7B).

A

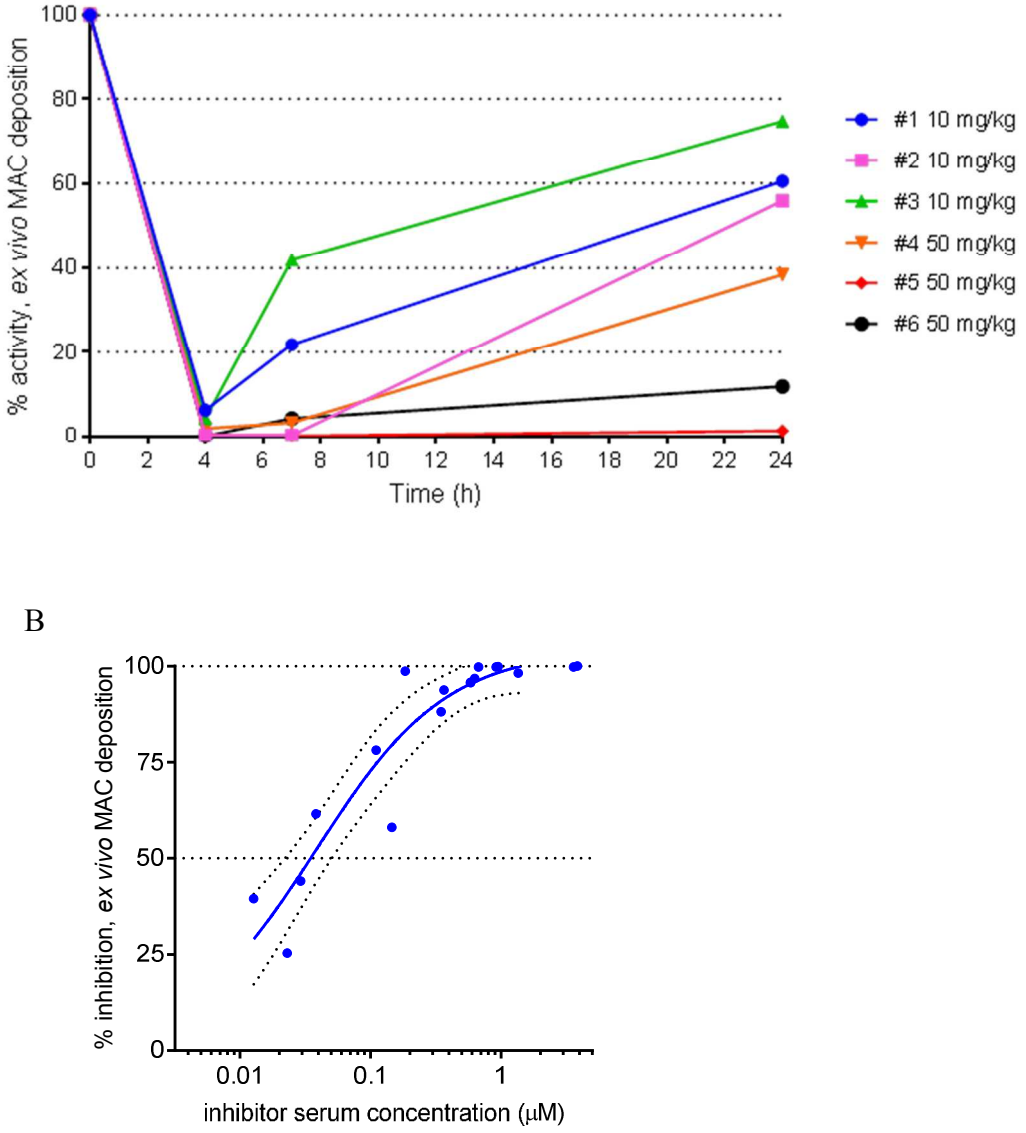

Figure 7: Inhibition of *ex vivo* MAC deposition after oral dosing of **2** to male cynomolgus monkeys. A single dose of **2** was administered by oral gavage at 10 mg/kg (n = 3) and 50 mg/kg (n = 3), respectively. Serum samples were obtained pre-dosing, and at 4, 7, and 24 hours after dosing, and complement activity was assessed with an *ex vivo* serum MAC deposition assay (A). The concentration of **2** in each sample relative to complement inhibition achieved was plotted in (B). The dotted lines indicate the 95% confidence band for the curve.

Conclusion

Merging the key pharmacophoric elements of two hits identified from SBDD and FBS approaches[7,8] led to the first sub-micromolar non-covalent FD inhibitor **7** which was selected as a lead compound. Subsequent structure-based optimization efforts focused on improving binding interactions to the S1, S1' and S2' key hot-spots of the FD active site in combination with optimizing the ADMET profile. Modifications of the P1' center proline were extensively explored and resulted in the bicyclic (1*R*,3*S*,5*R*)-2-aza-bicyclo[3.1.0]hexane scaffold, exemplified by **13**, as a preferred S1' binding motif for this class of FD inhibitors. Replacing the P2' anilide portion of the initial lead **7** by the 2-amino-6-bromo-pyridine motif provided inhibitors with markedly improved potencies in the 50% human whole blood MAC deposition functional assay. Finally, SAR tuning of the P1 indole-carboxamide portion in **26** identified the indazole-carboxamide motif, and switching concomitantly to the *N*-acetyl spacer, as in **2**, turned out to be beneficial for reducing CYP2D6 affinity. Compound **2** combines excellent *in vitro* potency, and distribution into ocular tissue with a clean *in vitro* selectivity and safety profile. Compound **2** demonstrated *in vivo* efficacy in a FD-knock in mouse model of complement activation and blocked systemic AP activity *ex vivo* after oral administration to cynomolgus monkeys. Compound **2** warranted further pre-clinical evaluation including *in vivo* efficacy, tolerability and safety.

EXPERIMENTAL SECTION

Experimental procedures and compound characterization for novel compounds

General chemistry information

Unless otherwise specified, all solvents and reagents were obtained from commercial suppliers and used without further drying or purification. (1*R*,3*S*,5*R*)-2-Aza-bicyclo[3.1.0]hexane-2,3-dicarboxylic acid 2-*tert*-butyl ester [*CAS* 197142-34-0] was purchased from Neptune Technotrade (USA). Phase separator were obtained from Biotage: Isolute Phase separator (Part Nr: 120-1908-F for 70 mL and Part Nr: 120-1909-J for 150 mL). Normal-phase flash chromatography was performed using Merck silica gel 60 (230-400 mesh), Merck Darmstadt, Germany. R_f values for thin layer chromatography (TLC) were determined using 5 x 10 cm TLC plates, silica gel F254, Merck, Darmstadt, Germany. ^{1}H NMR spectra were recorded on a Bruker Avance DPX 400 BBO spectrometer. High-resolution mass spectra (HRMS) measurements were performed by using electrospray ionization in positive ion modus after separation by liquid chromatography. The elemental composition was derived from the mass spectra acquired at the high resolution of about 30'000 on a Q Exactive Plus mass spectrometer (Thermo Scientific) coupled to an Ultimate 3000 UHPLC. High mass accuracy of <1.5 ppm was obtained by using a lock mass. Mass spectra (MS) and liquid chromatography mass spectra (LC−MS) were determined by using electrospray ionization in positive and negative ion modus using an Agilent 1100 series instrument. Purity was determined by analytical HPLC using an Agilent 1100 or 1200 series instrument and by integration of the area under the UV absorption curve at λ =254 nm or 214 nm wavelenght, all final compounds reported were at least 95% pure. t_R refers to retention time.

The following conditions (a to e) were used for analytical HPLC, if not indicated otherwise. Conditions a: Waters Symmetry C18; particle size 3.5 μm; column size 2.1 x 50 mm; eluent/gradient 20-95% CH_3CN/H_2O/3.5 min, 95% CH_3CN/2 min (CH_3CN and H_2O containing 0.1% TFA); flow rate 0.6 mL/min, column temperature 25 °C. Conditions b: Agilent Eclipse

XDB-C18; particle size 1.8 μm; column size 4.6 x 50 mm; eluent/gradient 20-100% CH_3CN/H_2O/6 min, 100% CH_3CN/1.5 min (CH_3CN and H_2O containing 0.1% of TFA); flow rate 1 mL/min. Conditions c: Waters X-Bridge C18; particle size 2.5 μm; column size; 3 x 50 mm; eluent/gradient 10-98% CH_3CN/H_2O/8.6 min; 98% CH_3CN/1.4 min (CH_3CN and H_2O containing 0.1% TFA); flow rate 1.4 mL/min; column temperature 40 °C. Conditions d: Waters Sunfire C18: particle size 2.5 μm; column size 3 x 30 mm; eluent/gradient 10-98% CH_3CN/H_2O/2.5 min; 98% CH_3CN/0.8 min (CH_3CN and H_2O containing 0.1% TFA); flow rate 1.4 mL/min. Conditions e: Agilent Eclipse XDB-C18; particle size 1.8 μm; column size: 4.6 x 50 mm; eluent/gradient 5-100% CH_3CN/H_2O/6 min, 100% CH_3CN/1.5 min (CH_3CN and H_2O containing 0.1% of TFA); flow rate: 1 mL/min.

General Procedure 1: Preparation of (*S*)-pyrrolidine-2-carboxylic acid (3-trifluoromethoxyphenyl)amide, trifluoroacetate salt (intermediate B (R = H), Scheme 1). Step A: To a mixture of *N*-Boc-L-proline (5.00 g, 23.2 mmol), 3-(trifluoromethoxy)aniline (3.73 mL, 27.9 mmol) and *N*,*N*,*N*′,*N*′-tetramethyl-O-(1*H*-benzotriazol-1-yl)uronium hexafluorophosphate (HBTU; 13.2 g, 34.8 mmol) in *N*,*N*-dimethyl-formamide (DMF, 60 mL) was added diisopropylethylamine (DIPEA; 7.95 mL, 46.5 mmol) and the resulting yellow solution was stirred at RT under a nitrogen atmosphere for 16 h. The solvent was evaporated under reduced pressure, the residue thus obtained was dissolved in EtOAc and the organics were washed with 1 N HCl. An aqueous saturated $NaHCO_3$ solution was added, the layers were separated and the aqueous phase was back-extracted twice with dichloromethane (CH_2Cl_2). The combined extracts were dried (Na_2SO_4), filtered and concentrated. The crude residue was purified by flash column chromatography on silica gel (c-hexane/EtOAc 3:1 to 2:1) to give (*S*)-2-(3-trifluoromethoxy-phenylcarbamoyl)-pyrrolidine-1-carboxylic acid *tert*-butyl ester

(intermediate **A** (R = H), Scheme 1) as a solid (8.52 g, yield 98%). TLC, R_f (c-hexane/EtOAc 1:1) 0.6. LC−MS (ESI, *m/z*) 397.1 $[M+Na]^+$, 275.2 $[MH\text{-}Boc]^+$, 373.3 $[M\text{-}H]^-$. t_R (HPLC, conditions a) 3.81 min (purity 95%). ^{1}H NMR (400 MHz, $CDCl_3$): δ (ppm) 9.80 (br s, 1H), 7.59 (s, 1H), 7.28 (m, 2H), 6.89 (m, 1H), 4.47 (m, 1H), 3.42 (m, 2H), 2.26 (m, 1H), 1.94 (m, 3H), 1.50 (s, 9H).

Step B: To a solution of (*S*)-2-(3-trifluoromethoxy-phenylcarbamoyl)-pyrrolidine-1-carboxylic acid *tert*-butyl ester (5.91 g, 15.8 mmol) in CH_2Cl_2 (10 mL) was added trifluoroacetic acid (TFA, 4.48 mL, 63.1 mmol) and the solution was stirred at RT for 24 h. The reaction mixture was concentrated under reduced pressure, diethylether (Et_2O) was added and the precipitate was filtered off to give crude (*S*)-pyrrolidine-2-carboxylic acid (3-trifluoromethoxy-phenyl)-amide trifluoroacetate salt as a brownish solid (5.04 g, yield 82%). LC−MS (ESI, *m/z*) 275.2 $[M+H]^+$, 273.3 $[M\text{-}H]^-$. t_R (HPLC, conditions a) 2.47 min (purity >95%). ^{1}H NMR (400 MHz, DMSO-d_6): δ (ppm) 10.8 (s, 1H), 9.27 (br s, 1H), 8.73 (br s, 1H), 7.79 (s, 1H), 7.50 (m, 2H), 7.13 (d, J = 6.8 Hz, 1H), 4.34 (m, 1H), 3.30 (m, 2H), 2.36 (m, 1H), 2.02 (m, 1H), 1.94 (m, 2H).

1-(2-((1R,3S,5R)-3-((6-bromopyridin-2-yl)carbamoyl)-2-azabicyclo[3.1.0]hexan-2-yl)-2-oxoethyl)-1H-indazole-3-carboxamide (2). The synthesis of compound **2** has been reported previously.[7]

(S)-Pyrrolidine-1,2-dicarboxylic acid 1-[(1-methyl-1H-indol-3-yl)-amide] 2-[(3-trifluoromethoxy-phenyl)-amide] (5). To a solution of (*S*)-pyrrolidine-2-carboxylic acid (3-trifluoromethoxy-phenyl)-amide trifluoro acetate salt (200 mg, 0.515 mmol; preparation described in General Procedure 1) and Et_3N (143 µL, 1.03 mmol) in THF (5 mL) was added a solution of 3-isocyanato-1-methyl-1*H*-indole **31** (133 mg, 0.77 mmol) in THF (5 mL) and stirring was continued for 5 h at RT under a nitrogen atmosphere. A solution of **31** (44 mg, 0.26

mmol) in THF (1 mL) was added again and the reaction mixture was stirred for another 16 h at RT. The mixture was poured into 1 N HCl and was extracted twice with EtOAc. The combined organics were dried (Na_2SO_4), filtered and concentrated. The residue was purified by flash column chromatography (SiO_2, solvent c-hexane/EtOAc 2:3) and subsequent prep HPLC (Waters SunFire C18-ODB; particle size 5 µm; column size 19 x 50 mm; eluent/gradient 20% CH_3CN/H_2O 2.5 min, 20-100% CH_3CN in H_2O for 10 min (CH_3CN and H_2O containing 0.1% HCOOH); flow rate 20 mL/min). The combined pure fractions were freeze-dried to afford **5** as a white solid (92 mg, yield 40%). TLC, R_f (c-hexane/EtOAc 2:3) 0.35. t_R (HPLC conditions a) 3.67 min (purity 95%). LC−MS (ESI, *m/z*) 447.3 $[M+H]^+$, 469.1 $[M+Na]^+$, 915.3 $[2M+Na]^+$, 445.3 $[M-H]^-$. ^1H NMR (400 MHz, $CDCl_3$): δ (ppm) 10.2 (s, 1H), 7.67 (br s, 1H), 7.45 (d, J = 7.8 Hz, 1H), 7.34-7.27 (m, 5H), 7.12 (t, J = 7.5 Hz, 1H), 6.91 (m, 1H), 6.23 (s, 1H), 4.78 (d, J = 7.6 Hz, 1H), 3.80 (s, 3H), 3.62 (m, 1H), 3.48 (m, 1H), 2.70 (dd, J = 12.5, 6.2 Hz, 1H), 2.32-2.13 (m, 2H), 1.93 (m, 1H). HRMS *m/z* (ESI) calcd for $C_{22}H_{21}F_3N_4O_3$ $[M+H]^+$ 447.16385; found, 447.16386).

General Procedure 2: Preparation of (*S*)-pyrrolidine-1,2-dicarboxylic acid 1-[(1-carbamoyl-1*H*-indol-3-yl)-amide] 2-[(3-trifluoromethoxy-phenyl)-amide] (7). To a solution of (*S*)-pyrrolidine-2-carboxylic acid (3-trifluoromethoxy-phenyl)-amide trifluoro acetate salt (328 mg, 0.845 mmol; preparation described in General Procedure 1) and Et_3N (353 µL, 2.53 mmol) in THF (7.5 mL) was added a suspension of **32** (170 mg, 0.845 mmol) in THF (7.5 mL). Stirring was continued at RT for 1 h under a nitrogen atmosphere. The reaction mixture was then poured into water and extracted twice with EtOAc. The combined organics were dried (Na_2SO_4), filtered and concentrated. The residue was purified by prep HPLC (Waters SunFire C18-ODB; particle size 5 µm; column size 19 x 50 mm; eluent/gradient 20% CH_3CN/H_2O 2.5 min, 20-

100% CH_3CN in H_2O for 10 min (CH_3CN and H_2O containing 0.1% HCOOH); flow rate 20 mL/min) to give, after lyophilization of the pure fractions, the title compound **7** as a white powder (173 mg, yield 43%). The enantiomeric excess (ee) >99% was determined by chiral HPLC and in comparison with **8**: t_R (Chiral Pack IC; particle size 5 μm; column size 4.6 x 250 mm; eluent heptane/isopropanol (85:15) containing 0.03% diethylamine; flow rate 1 mL/min; UV detection at 240 nm) 11.0 min (99.7% **7**), 14.04 min (0.3% **8**). TLC, R_f (c-hexane/EtOAc 1:2) 0.10. t_R (HPLC conditions c) 4.15 min (purity 99%). LC−MS (ESI, *m/z*) 476.2 $[M+H]^+$, 973.2 $[2M+Na]^+$. ^{1}H NMR (400 MHz, DMSO-d_6): δ (ppm) 10.3 (s, 1H), 8.25 (d, *J* = 8.6 Hz, 1H), 8.19 (s, 1H), 7.96 (s, 1H), 7.83 (s, 1H), 7.75 (d, *J* = 7.85 Hz, 1H), 7.51 (br d, *J* = 8.1 Hz, 1H), 7.42 (t, *J* = 8.2 Hz, 1H), 7.36 (br s, 2H), 7.23 (t, *J* = 7.5 Hz, 1H), 7.15 (t, *J* = 7.5 Hz, 1H), 7.02 (d, *J* = 7.85 Hz, 1H), 4.46 (m, 1H), 3.73 (m, 1H), 3.62 (m, 1H), 2.22 (m, 1H), 2.06 (m, 1H), 1.96 (m, 2H). HRMS *m/z* (ESI) calcd for $C_{22}H_{20}F_3N_5O_4$ $[M+H]^+$ 476.1540; found, 476.1539; calcd for $C_{22}H_{20}F_3N_5O_4Na$ $[M+Na]^+$ 498.1360; found, 498.1358; calcd for $C_{22}H_{20}F_3N_5O_4NH_4$ $[M+NH_4]^+$ 493.1806; found, 493.1805.

(*R*)-Pyrrolidine-1,2-dicarboxylic acid 1-[(1-carbamoyl-1*H*-indol-3-yl)-amide] 2-[(3-trifluoromethoxy-phenyl)-amide] (8). White solid (133 mg, yield 59%) obtained according to General Procedure 2 from (*R*)-*N*-(3-(trifluoromethoxy)phenyl)pyrrolidine-2-carboxamide trifluoro acetate salt (prepared according to General Procedure 1 by starting from (*R*)-1-(*tert*-butoxycarbonyl)pyrrolidine-2-carboxylic acid). t_R (HPLC conditions c) 4.08 min (>99% purity). Enantiomeric excess ee >99% (by chiral HPLC, as described for **7**). LC−MS (ESI, *m/z*) 476.4 $[M+H]^+$, 951.7 $[2M+H]^+$, 474.3 $[M-H]^-$, 949.7 $[2M-H]^-$. ^{1}H NMR (400 MHz, DMSO-d_6) δ (ppm) 10.3 (s, 1H), 8.27 (d, *J* = 8.3 Hz, 1H), 8.20 (s, 1H) 7.98 (s, 1H), 7.85 (s, 1H), 7.78 (d, *J* = 7.85 Hz, 1H), 7.55 (br d, *J* = 8.7 Hz, 1H), 7.45 (t, *J* = 8.2 Hz, 1H), 7.38 (br s, 2H), 7.26 (t, *J* = 7.7 Hz,

1H), 7.17 (t, *J* = 7.5 Hz, 1H), 7.04 (br d, *J* = 8.2 Hz, 1H), 4.49 (dd, *J* = 8.2, 3.9 Hz, 1H), 3.79-3.61 (m, 2H, overlapping with H_2O signal), 2.24 (m, 1H), 2.07 (m, 1H), 1.99 (m, 2H). HRMS *m*/*z* (ESI) calcd for $C_{22}H_{20}F_3N_5O_4$ $[M+H]^+$ 476.15402; found, 476.15364.

(2*S*,4*R*)-4-Methyl-pyrrolidine-1,2-dicarboxylic acid 1-[(1-carbamoyl-1*H*-indol-3-yl)-amide] 2-[(3-trifluoromethoxy-phenyl)-amide] (9). White solid (38 mg, yield 78%) obtained according to General Procedure 2 from (2*S*,4*R*)-4-methyl-*N*-(3-(trifluoromethoxy)phenyl)pyrrolidine-2-carboxamide trifluoro acetate salt (prepared from (2*S*,4*R*)-2-(3-trifluoromethoxy-phenylcarbamoyl)-4-methyl-pyrrolidine-1-carboxylic acid *tert*-butyl ester (**39**) prepared as described below). TLC, R_f (c-hexane/EtOAc 1:3) 0.45. t_R (HPLC conditions c) 4.51 min (purity 99%). LC−MS (ESI, *m/z*) 489.1 $[M-H]^-$, 445.0 $[M-CONH_2]^-$. ^{1}H NMR (400 MHz, DMSO-d_6): δ (ppm) 10.3 (s, 1H), 8.27 (d, *J* = 8.1 Hz, 1H), 8.17 (s, 1H), 7.98 (s, 1H), 7.85 (s, 1H), 7.79 (d, *J* = 8.1 Hz, 1H), 7.53 (d, *J* = 8.3 Hz, 1H), 7.45 (t, *J* = 8.5 Hz, 1H), 7.38 (br s, 2H), 7.26 (t, *J* = 7.5 Hz, 1H), 7.17 (t, *J* = 7.5 Hz, 1H), 7.04 (d, *J* = 8.1 Hz, 1H), 4.54 (d, *J* = 8.1 Hz, 1H), 3.94 (t, *J* = 8.2 Hz, 1H), 3.19 (t, *J* = 8.4 Hz, 1H), 2.56 (m, 1H), 2.07 (m, 1H), 1.90 (m, 1H), 1.09 (t, *J* = 6.4 Hz, 3H). HRMS *m*/*z* (ESI) calcd for $C_{23}H_{22}F_3N_5O_4$ $[M+H]^+$ 490.16967; found, 490.16924.

(2*S*,4*S*)-4-Methyl-pyrrolidine-1,2-dicarboxylic acid 1-[(1-carbamoyl-1*H*-indol-3-yl)-amide] 2-[(3-trifluoromethoxy-phenyl)-amide] (10). White solid (29 mg, yield 59%) obtained according to General Procedure 2 from (2*S*,4*S*)-4-methyl-*N*-(3-(trifluoromethoxy)phenyl)-pyrrolidine-2-carboxamide trifluoro acetate salt (prepared from (2*S*,4*S*)-2-(3-trifluoromethoxy-phenylcarbamoyl)-4-methyl-pyrrolidine-1-carboxylic acid *tert*-butyl ester (**40**), prepared as described below). TLC, R_f (c-hexane/EtOAc 1:3) 0.45. t_R (HPLC conditions c) 4.39 min (purity 99%). LC−MS (ESI, *m/z*) 490.3 $[M+H]^+$, 976.6 $[2M+H]^+$, 488.3 $[M-H]^-$, 977.7 $[2M-H]^-$, 1023.8 $[2M-CONH_2]^-$. ^{1}H NMR (400 MHz, DMSO-d_6): δ (ppm) 10.4 (s, 1H), 8.27 (d, *J* = 8.3 Hz, 1H),

8.24 (s, 1H), 7.98 (s, 1H), 7.86 (s, 1H), 7.80 (d, *J* = 7.8 Hz, 1H), 7.54 (d, *J* = 8.3 Hz, 1H), 7.45 (t, *J* = 8.2 Hz, 1H), 7.37 (br s, 2H), 7.25 (t, *J* = 7.7 Hz, 1H), 7.16 (t, *J* = 7.6 Hz, 1H), 7.04 (d, *J* = 8.2 Hz, 1H), 4.45 (t, *J* = 7.8 Hz, 1H), 3.92 (t, *J* = 8.2 Hz, 1H), 3.22 (t, *J* = 9.4 Hz, 1H), 2.42 (m, 2H), 1.53 (m, 1H), 1.12 (t, *J* = 5.9 Hz, 3H). HRMS *m/z* (ESI) calcd for $C_{23}H_{22}F_3N_5O_4$ $[M+H]^+$ 490.16967; found, 490.16929.

(1*S*,2*S*,5*R*)-3-Aza-bicyclo[3.1.0]hexane-2,3-dicarboxylic acid 3-[(1-carbamoyl-1*H*-indol-3-yl)-amide] 2-[(3-trifluoromethoxy-phenyl)-amide] (11). Pale yellowish solid (64 mg, yield 53%) obtained according to General Procedure 2 from (1*S*,2*S*,5*R*)-*N*-(3-(trifluoromethoxy)-phenyl)-3-azabicyclo[3.1.0]hexane-2-carboxamide trifluoro acetate salt (prepared according to General Procedure 1 by starting from (1*S*,2*S*,5*R*)-3-(*tert*-butoxycarbonyl)-3-azabicyclo[3.1.0]hexane-2-carboxylic acid). t_R (HPLC conditions c) 4.27 min (purity >99%). LC−MS (ESI, *m/z*) 488.2 $[M+H]^+$, 510.1 $[M+Na]^+$. ^{1}H NMR (400 MHz, DMSO-d_6): δ (ppm) 10.6 (s, 1H), 8.26 (d, *J* = 8.3 Hz, 1H), 8.17 (s, 1H), 7.95 (s, 1H), 7.88 (br s, 1H), 7.74 (d, *J* = 7.85 Hz, 1H), 7.51 (m, 1H), 7.46 (t, *J* = 8.2 Hz, 1H), 7.37 (br s, 2H), 7.25 (t, *J* = 7.7 Hz, 1H), 7.17 (t, *J* = 7.5 Hz, 1H), 7.05 (d, *J* = 8.1 Hz, 1H), 4.58 (s, 1H), 3.88 (d, *J* = 9.25 Hz, 1H), 3.79 (dd, *J* = 9.25, 4.0 Hz, 1H), 1.78 (m, 1H), 1.72 (m, 1H), 0.84 (m, 1H), 0.37 (m, 1H). HRMS *m/z* (ESI) calcd for $C_{23}H_{20}F_3N_5O_4$ $[M+H]^+$ 488.1540; found, 488.1539; calcd for $C_{23}H_{21}N_4O_4F_3Na$ $[M+Na]^+$ 510.1360; found, 510.1358.

(*S*)-Piperidine-1,2-dicarboxylic acid 1-[(1-carbamoyl-1*H*-indol-3-yl)-amide] 2-[(3-trifluoromethoxy-phenyl)-amide] (12). White solid (16 mg, yield 16%) obtained according to General Procedure 2 from (*S*)-*N*-(3-(trifluoromethoxy)phenyl)piperidine-2-carboxamide trifluoro acetate salt (prepared according to General Procedure 1 by starting from (*S*)-1-(*tert*-butoxycarbonyl)piperidine-2-carboxylic acid). TLC, R_f (c-hexane/EtOAc 1:2) 0.21. t_R (HPLC

conditions c) 4.68 min (purity 98%). LC−MS (ESI, *m/z*) 490.1 $[M+H]^+$, 1001.2 $[2M+Na]^+$, 488.1 $[M-H]^-$. ^{1}H NMR (400 MHz, DMSO-d_6): δ (ppm) 10.3 (s, 1H), 8.51 (s, 1H), 8.25 (d, J = 8.10 Hz, 1H), 7.98 (s, 1H), 7.82 (s, 1H), 7.76 (d, J = 8.10 Hz, 1H), 7.54 (d, J = 8.35 Hz, 1H), 7.42 (t, J = 8.3 Hz, 1H), 7.37 (br s, 2H), 7.23 (t, J = 7.6 Hz, 1H), 7.15 (t, J = 7.5 Hz, 1H), 7.02 (d, J = 8.1 Hz, 1H), 4.89 (m, 1H), 4.06 (d, J = 12.1 Hz, 1H), 3.47 (t, J = 11.9 Hz, 1H), 2.15 (d, J = 13.7 Hz, 1H), 1.75 (m, 2H), 1.34 (m, 1H), 1.50 (m, 1H), 1.38 (m, 1H). HRMS *m/z* (ESI) calcd for $C_{23}H_{22}F_3N_5O_4$ $[M+H]^+$ 490.16967; found, 490.16959.

(1*R*,3*S*,5*R*)-2-Aza-bicyclo[3.1.0]hexane-2,3-dicarboxylic acid 2-[(1-carbamoyl-1*H*-indol-3-yl)-amide] 3-[(3-trifluoromethoxy-phenyl)-amide] (13). White solid (640 mg, yield 89%) obtained according to General Procedure 2 from (1*R*,3*S*,5*R*)-*N*-(3-(trifluoromethoxy)phenyl)-2-azabicyclo[3.1.0]hexane-3-carboxamide trifluoro acetate salt (prepared according to the General Procedure 1 by starting from (1*R*,3*S*,5*R*)-2-(*tert*-butoxycarbonyl)-2-azabicyclo[3.1.0]hexane-3-carboxylic acid [CAS 197142-34-0; Neptune Technotrade, USA]). TLC, R_f (c-hexane/EtOAc 1:2) 0.40. LC−MS (ESI, *m/z*) 488 $[M+H]^+$, 997.2 $[2M+Na]^+$, 486.1 $[M-H]^-$, 443.2 $[M-CONH_2]^-$. t_R (HPLC conditions c) 4.29 min (purity >99%). t_R (HPLC conditions d) 2.1 min (purity >99%). ^{1}H NMR (400 MHz, DMSO-d_6) δ (ppm) 10.2 (s, 1H), 8.66 (s, 1H), 8.27 (d, J = 8.3 Hz, 1H), 8.01 (s, 1H), 7.84 (s, 1H), 7.81 (d, J = 7.8 Hz, 1H), 7.56 (d, J = 8.3 Hz, 1H), 7.44 (t, J = 8.2 Hz, 1H), 7.39 (br s, 2H), 7.27 (t, J = 7.6 Hz, 1H), 7.20 (t, J = 7.5 Hz, 1H), 7.04 (d, J = 8.3 Hz, 1H), 4.21 (t, J = 8.1 Hz, 1H), 3.94 (m, 1H), 2.37 (dd, J = 13.0, 8.8 Hz, 1H), 2.19 (m, 1H), 1.83 (m, 1H), 0.83 (m, 1H), 0.59 (m, 1H). ^{13}C NMR (150 MHz, DMSO-d_6): δ (ppm) 170.7, 156.0, 152.9, 148.4, 140.8, 133.6, 130.4, 124.3, 124.0, 121.0, 120.0 (q, J = 255 Hz, CF_3), 119.2, 118.6, 117.7, 115.2, 115.15, 114.5, 111.1, 61.5, 36.3, 31.5, 16.4, 13.9. HRMS *m/z* (ESI) calcd for $C_{23}H_{20}F_3N_5O_4$

$[M+H]^+$ 488.1540; found, 488.1539; calcd for $C_{23}H_{20}F_3N_5O_4Na$ $[M+Na]^+$ 510.1360; found, 510.1358.

(2*S*,4*R*)-4-Fluoro-pyrrolidine-1,2-dicarboxylic acid 1-[(1-carbamoyl-1*H*-indol-3-yl)-amide] 2-[(3-trifluoromethoxy-phenyl)-amide] (14). White solid (67 mg, yield 68%) obtained according to General Procedure 2 from (2*S*,4*R*)-4-fluoro-*N*-(3-(trifluoromethoxy)phenyl)-pyrrolidine-2-carboxamide trifluoro acetate salt (prepared according to General Procedure 1 by starting from (2*S*,4*R*)-1-(*tert*-butoxycarbonyl)-4-fluoropyrrolidine-2-carboxylic acid). TLC, R_f (c-hexane/EtOAc 1:2) 0.35. LC−MS (ESI, *m/z*) 494.0 $[M+H]^+$, 492.1 $[M-H]^-$. t_R (HPLC conditions c) 4.00 min (purity >99%). ^{1}H NMR (400 MHz, DMSO-d_6): δ (ppm) 10.5 (s, 1H), 8.44 (s, 1H), 8.27 (d, *J* = 10.1 Hz, 1H), 7.99 (s, 1H), 7.85 (s, 1H), 7.78 (d, *J* = 7.8 Hz, 1H), 7.53 (d, *J* = 7.6 Hz, 1H), 7.46 (t, *J* = 8.2 Hz, 1H), 7.38 (br s, 2H), 7.26 (t, *J* = 7.7 Hz, 1H), 7.17 (t, *J* = 7.5 Hz, 1H), 7.05 (br d, *J* = 8.1 Hz, 1H), 5.51 (br d, *J* = 53 Hz, 1H), 4.64 (dd, *J* = 9.0, 7.6 Hz, 1H), 4.07-3.85 (m, 2H), 2.56 (m, 1H), 2.18 (m, 1H). HRMS *m/z* (ESI) calcd for $C_{22}H_{19}F_4N_5O_4$ $[M+H]^+$ 494.14459; found, 494.14423.

(2*S*,4*S*)-4-Fluoro-pyrrolidine-1,2-dicarboxylic acid 1-[(1-carbamoyl-1*H*-indol-3-yl)-amide] 2-[(3-trifluoromethoxy-phenyl)-amide] (15). White solid (42 mg, yield 69%) obtained according to General Procedure 2 from (2*S*,4*S*)-4-fluoro-*N*-(3-(trifluoromethoxy)phenyl)-pyrrolidine-2-carboxamide trifluoro acetate salt (prepared according to General Procedure 1 by starting from (2*S*,4*S*)-1-(*tert*-butoxycarbonyl)-4-fluoropyrrolidine-2-carboxylic acid using CH_2Cl_2 instead of DMF in step A). R_f (c-hexane/EtOAc 1:3) 0.2. t_R (HPLC conditions c) 3.97 min (purity >99%). LC−MS (ESI, *m/z*) 494 $[M+H]^+$. ^{1}H NMR (400 MHz, DMSO-d_6): δ (ppm) 10.2 (s, 1H), 8.30 (s, 1H), 8.28 (d, *J* = 8.3 Hz, 1H), 8.01 (s, 1H), 7.83 (s, 1H), 7.81 (br d, *J* = 8.3 Hz, 1H), 7.58 (m, 1H), 7.45 (t, *J* = 8.3 Hz, 1H), 7.41 (br s, 2H), 7.26 (t, *J* = 7.7 Hz, 1H), 7.18 (t, *J*

= 7.5 Hz, 1H), 7.05 (m, 1H), 5.45 (br d, *J* = 54 Hz, 1H), 4.6 (m, 1H), 4.09-3.87 (m, 2H), 2.62-2.35 (m, 2H; overlapping with DMSO signal). HRMS *m/z* (ESI) calcd for $C_{22}H_{19}F_4N_5O_4$ $[M+H]^+$ 494.14459; found, 494.14396.

(*S*)-4,4-Difluoro-pyrrolidine-1,2-dicarboxylic acid 1-[(1-carbamoyl-1*H*-indol-3-yl)-amide] 2-[(3-trifluoromethoxy-phenyl)-amide] (16). Pale brownish solid (66 mg, yield 52%) obtained according to General Procedure 2 from (*S*)-4,4-difluoro-*N*-(3-(trifluoromethoxy)phenyl)-pyrrolidine-2-carboxamide trifluoro acetate salt (prepared according to the General Procedure 1 by starting from (*S*)-1-(*tert*-butoxycarbonyl)-4,4-difluoropyrrolidine-2-carboxylic acid). LC−MS (ESI, *m/z*) 512.2 $[M+H]^+$, 510.1 $[M-H]^-$. t_R (HPLC conditions c) 4.37 min (purity >99%). ^{1}H NMR (400 MHz, DMSO-d_6): δ (ppm) 10.5 (s, 1H), 8.48 (s, 1H), 8.28 (d, *J* = 8.2 Hz, 1H), 8.00 (s, 1H), 7.83 (br s, 1H), 7.78 (d, *J* = 7.8 Hz, 1H), 7.54 (d, *J* = 7.6 Hz, 1H), 7.47 (t, *J* = 8.2 Hz, 1H), 7.43 (br s, 2H), 7.27 (t, *J* = 7.7 Hz, 1H), 7.19 (t, *J* = 7.2 Hz, 1H), 7.07 (br d, *J* = 8.1 Hz, 1H), 4.75 (dd, *J* = 9.0, 5.6 Hz, 1H), 4.21 (m, 2H), 2.93 (m, 1H), 2.58 (m, 1H). HRMS *m/z* (ESI) calcd for $C_{22}H_{18}F_5N_5O_4$ $[M+H]^+$ 512.1352; found, 512.1350; calcd for $C_{22}H_{18}F_5N_5O_4Na$ $[M+Na]^+$ 534.1171; found, 534.1169; calcd for $C_{22}H_{18}F_5N_5O_4NH_4$ $[M+NH_4]^+$ 529.1617; found, 529.1617.

(2*S*,4*S*)-4-Hydroxy-pyrrolidine-1,2-dicarboxylic acid 1-[(1-carbamoyl-1*H*-indol-3-yl)-amide] 2-[(3-trifluoromethoxy-phenyl)-amide] (17). White solid (50 mg, yield 36%) obtained according to General Procedure 2 from (2*S*,4*S*)-4-hydroxy-*N*-(3-(trifluoromethoxy)phenyl)-pyrrolidine-2-carboxamide trifluoro acetate salt (prepared according to General Procedure 1 by starting from (2*S*,4*S*)-1-(*tert*-butoxycarbonyl)-4-hydroxypyrrolidine-2-carboxylic acid). t_R (HPLC conditions c) 3.65 min (purity 98%). LC−MS (ESI, *m/z*) 492.1 $[M+H]^+$, 514.2 $[M+H]^+$, 490.1 $[M-H]^-$. ^{1}H NMR (400 MHz, DMSO-d_6): δ (ppm) 10.3 (s, 1H), 8.27 (m, 2H), 7.99 (s, 1H), 7.85 (br s, 1H), 7.80 (d, *J* = 7.8 Hz, 1H), 7.56 (br d, *J* = 8.3 Hz, 1H), 7.46 (t, *J* = 8.2 Hz, 1H),

7.39 (br, 2H), 7.26 (t, *J* = 7.6 Hz, 1H), 7.18 (t, *J* = 7.5 Hz, 1H), 7.06 (br d, *J* = 8.10 Hz, 1H), 5.30 (m, 1H), 4.49 (dd, *J* = 8.4, 5.9 Hz, 1H), 4.40 (m, 1H), 3.86 (dd, *J* = 10.0, 5.7 Hz, 1H), 3.56 (dd, *J* = 9.85, 4.8 Hz, 1H), 2.46 (m, 1H), 1.91 (m, 1H). HRMS *m*/*z* (ESI) calcd for $C_{22}H_{20}F_3N_5O_5$ $[M+H]^+$ 492.14893; found, 492.14880.

(2*S*,4*S*)-4-Amino-pyrrolidine-1,2-dicarboxylic acid 1-[(1-carbamoyl-1*H*-indol-3-yl)-amide] 2-[(3-trifluoromethoxy-phenyl)-amide], formate salt (18).

(2*S*,4*S*)-4-*N*-Fmoc-amino-pyrrolidine-1,2-dicarboxylic acid 1-[(1-carbamoyl-1*H*-indol-3-yl)-amide] 2-[(3-trifluoromethoxy-phenyl)-amide] was prepared according to General Procedure 2 from (9*H*-fluoren-9-yl)methyl ((3*S*,5*S*)-5-((3-(trifluoromethoxy)phenyl)carbamoyl)pyrrolidin-3-yl)carbamate trifluoro acetate salt (prepared according to General Procedure 1 by starting from (4*S*)-4-*N*-Fmoc-amino-1-Boc-L-proline), White solid (472 mg, yield 59%). TLC, R_f (AcOEt) 0.55. t_R (HPLC conditions a) 4.17 min (purity >95%). MS (LC/MS): 713.2 $[M+H]^+$, 735.1 $[M+Na]^+$.

(2*S*,4*S*)-4-*N*-Fmoc-amino-pyrrolidine-1,2-dicarboxylic acid 1-[(1-carbamoyl-1*H*-indol-3-yl)-amide] 2-[(3-trifluoromethoxy-phenyl)-amide] (380 mg, 0.533 mmol) was dissolved in a 20% solution of piperidine in DMF (2 mL). The mixture was stirred for 1 h at RT and then directly purified by prep HPLC (Interchrom C18-ODB; particle size 10 μm; column size 28 x 250 mm; eluent/gradient 5% CH_3CN in H_2O 2.5 min, then 5% to 100 % CH_3CN in H_2O in 32.5 min (CH_3CN and H_2O containing 0.1% HCOOH); flow rate 40 mL/min). To the combined fractions containing the title compound was added 1 N NaOH and the aqueous layer was extracted with EtOAc three times. The combined organics were dried (Na_2SO_4), filtered and concentrated. The residue thus obtained was then purified by prep HPLC (Water SunFire C18-ODB; particle size 5 μm; column size 19 x 50 mm; eluent/gradient 5% to 60% CH_3CN in H_2O for 18 min (CH_3CN

and H_2O containing 0.1% HCOOH); flow rate 20 mL/min) and the combined pure fractions were freeze-dried to give **18** as a white solid (138 mg, 48%). t_R (HPLC conditions a) 2.73 min (purity >99%). LC−MS (ESI, *m/z*) 491.2 $[M+H]^+$, 489.1 $[M-H]^-$. ^1H NMR (400 MHz, DMSO-d_6): δ (ppm) 8.28 (s, 1H), 8.25 (d, *J* = 7.8 Hz, 1H), 8.21 (s, 1H), 7.97 (s, 1H), 7.82 (s, 1H), 7.75 (d, *J* = 7.6 Hz, 1H), 7.49 (d, *J* = 8.1 Hz, 1H), 7.43 (t, *J* = 8.1 Hz, 1H), 7.37 (br s, 2H), 7.23 (t, *J* = 7.6 Hz, 1H), 7.15 (t, *J* = 7.0 Hz, 1H), 7.04 (d, *J* = 7.6 Hz, 1H), 4.42 (m, 1H), 3.80 (m, 1H), 3.63 (m, 1H), 3.45 (m, 1H; overlapping with H_2O signal), 2.24 (m, 1H; overlaping with DMSO signal), 1.81 (m, 1H). HRMS *m/z* (ESI) calcd for $C_{22}H_{21}F_3N_6O_4$ $[M+H]^+$ 491.1649; found, 491.1648.

(1*R*,3*S*,5*R*)-2-Aza-bicyclo[3.1.0]hexane-2,3-dicarboxylic acid 2-[(1-carbamoyl-1*H*-indol-3-yl)-amide] 3-[(3-difluoromethoxy-phenyl)-amide] (19). White solid (39 mg, yield 61%) obtained according to General Procedure 2 from (1*R*,3*S*,5*R*)-*N*-(3-(difluoromethoxy)phenyl)-2-azabicyclo[3.1.0]hexane-3-carboxamide trifluoroacetate salt (prepared according to the General Procedure 1 by starting from (1*R*,3*S*,5*R*)-2-(*tert*-butoxycarbonyl)-2-azabicyclo[3.1.0]hexane-3-carboxylic acid and 3-(difluoromethoxy)aniline and using CH_2Cl_2 as the solvent in step A). t_R (HPLC conditions c) 3.80 min (purity 98%). LC−MS (ESI, *m/z*) 470.0 $[M+H]^+$, 468.9 $[M-H]^-$, 425.0 $[M-CONH_2]^-$. ^1H NMR (400 MHz, DMSO-d_6): δ (ppm) 10.1 (s, 1H), 8.65 (s, 1H), 8.28 (d, *J* = 8.2 Hz, 1H), 8.01 (s, 1H), 7.81 (d, *J* = 7.7 Hz, 1H), 7.63 (s, 1H), 7.44 (m, 1H), 7.37 (br s, 2H), 7.35 (t, *J* = 8.2 Hz, 1H), 7.27 (m, 2H), 7.20 (m, 1H), 7.20 (t, *J* = 74 Hz, 1H), 6.87 (dd, *J* = 8.2, 2.2 Hz, 1H), 4.21 (t, *J* = 8.0 Hz, 1H), 3.94 (m, 1H), 2.36 (dd, *J* = 13.0, 8.9 Hz, 1H), 2.17 (m, 1H), 1.83 (m, 1H), 0.85 (m, 1H), 0.59 (m, 1H). HRMS *m/z* (ESI) calcd for $C_{23}H_{21}F_2N_5O_4$ $[M+H]^+$ 470.16344; found, 470.16403.

(1*R*,3*S*,5*R*)-2-Aza-bicyclo[3.1.0]hexane-2,3-dicarboxylic acid 2-[(1-carbamoyl-1*H*-indol-3-yl)-amide] 3-[(3-methoxy-phenyl)-amide] (20). White solid (55 mg, yield 66%) obtained

according to General Procedure 2 from (1*R*,3*S*,5*R*)-*N*-(3-methoxyphenyl)-2-azabicyclo[3.1.0]hexane-3-carboxamide trifluoroacetate salt (prepared according to the General Procedure 1 by starting from (1*R*,3*S*,5*R*)-2-(*tert*-butoxycarbonyl)-2-azabicyclo[3.1.0]hexane-3-carboxylic acid and 3-methoxyaniline and using CH_2Cl_2 as the solvent in step A). t_R (HPLC conditions c) 3.33 min (purity 97%). LC−MS (ESI, *m/z*) 434.0 $[M+H]^+$, 388.9 $[M-CONH_2]^-$. ^1H NMR (400 MHz, DMSO-d_6): δ (ppm) 9.89 (s, 1H), 8.64 (s, 1H), 8.28 (d, *J* = 8.2 Hz, 1H), 8.02 (s, 1H), 7.81 (d, *J* = 7.7 Hz, 1H), 7.39 (br s, 2H), 7.35 (m, 1H), 7.27 (m, 1H), 7.23-7.16 (m, 3H), 6.63 (m, 1H), 4.21 (t, *J* = 8.0 Hz, 1H), 3.93 (m, 1H), 3.73 (s, 3H), 2.35 (dd, *J* = 12.9, 8.9 Hz, 1H), 2.18 (m, 1H), 1.81 (m, 1H), 0.85 (m, 1H), 0.58 (m, 1H). HRMS *m*/*z* (ESI) calcd for $C_{23}H_{23}N_5O_4$ $[M+H]^+$ 434.18228; found, 434.18243.

(1*R*,3*S*,5*R*)-2-Aza-bicyclo[3.1.0]hexane-2,3-dicarboxylic acid 2-[(1-carbamoyl-1*H*-indol-3-yl)-amide] 3-[(3-chlorophenyl)-amide] (21). White solid (47 mg, 61%) obtained according to General Procedure 2 from (1*R*,3*S*,5*R*)-*N*-(3-chlorophenyl)-2-azabicyclo[3.1.0]hexane-3-carboxamide trifluoroacetate salt (prepared according to the General Procedure 1 by starting from (1*R*,3*S*,5*R*)-2-(*tert*-butoxycarbonyl)-2-azabicyclo[3.1.0]hexane-3-carboxylic acid and 3-chloroaniline and using CH_2Cl_2 as the solvent in step A). t_R (HPLC conditions b) 4.12 min (purity >95%). LC−MS (ESI, *m/z*) 438.0/440.0 $[M+H]^+$, 437.8 $[M-H]^-$, 393/395 $[M-CONH_2]^-$. ^1H NMR (400 MHz, DMSO-d_6): δ (ppm) 10.1 (s, 1H), 8.66 (s, 1H), 8.29 (d, *J* = 8.2 Hz, 1H), 8.01 (s, 1H), 7.86 (t, *J* = 1.9 Hz, 1H), 7.81 (d, *J* = 7.6 Hz, 1H), 7.51 (m, 1H), 7.39 (br s, 2H), 7.34 (t, *J* = 8.1 Hz, 1H), 7.27 (m, 1H), 7.20 (m, 1H), 7.11 (m, 1H), 4.20 (t, *J* = 8.0 Hz, 1H), 3.94 (m, 1H), 2.37 (dd, *J* = 12.9, 8.8 Hz, 1H), 2.17 (m, 1H), 1.82 (m, 1H), 0.85 (m, 1H), 0.60 (m, 1H). HRMS *m*/*z* (ESI) calcd for $C_{22}H_{21}O_3N_5{}^{35}Cl$ $[M+H]^+$ 438.13274; found, 438.13272.

(1*R*,3*S*,5*R*)-2-Aza-bicyclo[3.1.0]hexane-2,3-dicarboxylic acid 3-[(3-bromophenyl)amide] 2-[(1-carbamoyl-1*H*-indol-3-yl)amide] (22). White solid (45 mg, yield 59%) obtained according to General Procedure 2 from (1*R*,3*S*,5*R*)-*N*-(3-bromophenyl)-2-azabicyclo[3.1.0]hexane-3-carboxamide trifluoroacetate salt (prepared according to the General Procedure 1 by starting from (1*R*,3*S*,5*R*)-2-(*tert*-butoxycarbonyl)-2-azabicyclo[3.1.0]hexane-3-carboxylic acid and 3-bromoaniline and using CH_2Cl_2 as the solvent in step A). t_R (HPLC conditions b) 4.20 min (purity >95%), LC−MS (ESI, *m/z*) 481.9/483.0 $[M+H]^+$, 481.9/482.8 $[M-H]^-$, 436.9/438.9 $[M-CONH_2]^-$. ^{1}H NMR (400 MHz, DMSO-d_6): δ (ppm) 10.1 (s, 1H), 8.65 (s, 1H), 8.29 (d, *J* = 8.2 Hz, 1H), 8.01 (m, 2H), 7.81 (d, *J* = 7.7 Hz, 1H), 7.55 (m, 1H), 7.39 (br s, 2H), 7.30-7.23 (m, 3H), 7.20 (m, 1H), 4.19 (t, *J* = 8.1 Hz, 1H), 3.94 (m, 1H), 2.36 (dd, *J* = 13.0, 9.0 Hz, 1H), 2.18 (m, 1H), 1.82 (m, 1H), 0.85 (m, 1H), 0.60 (m, 1H). HRMS *m/z* (ESI) calcd for $C_{22}H_{21}O_3N_5{}^{79}Br$ $[M+H]^+$ 482.08223; found, 482.08221.

(1*R*,3*S*,5*R*)-2-Aza-bicyclo[3.1.0]hexane-2,3-dicarboxylic acid 2-[(1-carbamoyl-1*H*-indol-3-yl)-amide] 3-[(2-fluoro-3-trifluoromethoxy-phenyl)-amide] (23). White solid (270 mg, yield 63%) obtained according to General Procedure 2 from (1*R*,3*S*,5*R*)-*N*-(2-fluoro-3-(trifluoromethoxy)phenyl)-2-azabicyclo[3.1.0]hexane-3-carboxamide trifluoroacetate salt (prepared according to the General Procedure 1 by starting from (1*R*,3*S*,5*R*)-2-(*tert*-butoxycarbonyl)-2-azabicyclo[3.1.0]hexane-3-carboxylic acid and 2-fluoro-3-(trifluoromethoxy)aniline [CAS 1159512-64-7] and heating the reaction mixture at 70°C in step A). t_R (HPLC conditions b) 4.46 min (purity 99%). LC−MS (ESI, *m/z*) 506 $[M+H]^+$. ^{1}H NMR (400 MHz, DMSO-d_6): δ (ppm) 9.98 (s, 1H), 8.68 (s, 1H), 8.29 (d, *J* = 8.3 Hz, 1H), 8.01 (s, 1H), 7.95 (m, 1H), 7.80 (d, *J* = 7.8 Hz, 1H), 7.42 (br s, 2H), 7.33-7.26 (m, 3H), 7.20 (t, *J* = 7.1 Hz, 1H), 4.40 (dd, *J* = 8.5, 7.3 Hz, 1H), 3.91 (m, 1H), 2.38 (dd, *J* = 12.8, 8.9 Hz, 1H), 2.23 (m, 1H),

1.83 (m, 1H), 0.86 (m, 1H), 0.59 (m, 1H). HRMS *m/z* (ESI) calcd for $C_{23}H_{20}O_4N_5F_4$ $[M+H]^+$ 506.14459; found, 506.14471.

(1*R*,3*S*,5*R*)-2-Aza-bicyclo[3.1.0]hexane-2,3-dicarboxylic acid 2-[(1-carbamoyl-1*H*-indol-3-yl)-amide] 3-[(2-fluoro-3-trifluoromethyl-phenyl)-amide] (24). White solid (45 mg, yield 72%) obtained according to General Procedure 2 from (1*R*,3*S*,5*R*)-*N*-(2-fluoro-3-(trifluoromethyl)phenyl)-2-azabicyclo[3.1.0]hexane-3-carboxamide trifluoroacetate salt (prepared according to the General Procedure 1 by starting from (1*R*,3*S*,5*R*)-2-(*tert*-butoxycarbonyl)-2-azabicyclo[3.1.0]hexane-3-carboxylic acid and 2-fluoro-3-(trifluoromethyl)aniline and using CH_2Cl_2 as the solvent in step A). t_R (HPLC conditions b) 4.39 min (purity 97%). LC−MS (ESI, *m/z*) 490 $[M+H]^+$. ^{1}H NMR (400 MHz, DMSO-d_6): δ (ppm) 10.0 (s, 1H), 8.68 (s, 1H), 8.29 (d, *J* = 8.3 Hz, 1H), 8.21 (t, *J* = 7.5 Hz, 1H), 8.05 (s, 1H), 7.80 (d, *J* = 7.8 Hz, 1H), 7.53 (t, *J* = 6.9 Hz, 1H), 7.43 (br s, 2H), 7.40 (t, *J* = 8.0 Hz, 1H), 7.28 (t, *J* = 7.7 Hz, 1H), 7.20 (t, *J* = 7.5 Hz, 1H), 4.40 (dd, *J* = 8.6, 7.3 Hz, 1H), 3.90 (m, 1H), 2.39 (dd, *J* = 12.9, 8.9 Hz, 1H), 1.83 (m, 1H), 0.87 (m, 1H), 0.61 (m, 1H). HRMS *m/z* (ESI) calcd for $C_{23}H_{20}O_3N_5F_3$ $[M+H]^+$ 490.14968; found, 490.14981.

(1*R*,3*S*,5*R*)-2-Azabicyclo[3.1.0]hexane-2,3-dicarboxylic acid 2-[(1-carbamoyl-1*H*-indol-3-yl)-amide] 3-[(6-trifluoromethyl-pyridin-2-yl)-amide] (25). To a solution of (1*R*,3*S*,5*R*)-2-aza-bicyclo[3.1.0]hexane-2,3-dicarboxylic acid 2-*tert*-butyl ester ([CAS 197142-34-0; Neptune Technotrade, USA; 400 mg, 1.76 mmol) in dry CH_2Cl_2 (9.6 mL) was added 1-chloro-*N*,*N*,2-trimethylpropenylamine (259 mg, 1.94 mmol) at 0 °C under a nitrogen atmosphere. Formation of the acyl chloride intermediate was monitored by TLC after quenching of an aliquot with MeOH to form the corresponding methyl ester. After completion of the reaction (2 h), 6-(trifluoromethyl)pyridin-2-amine (314 mg, 1.94 mmol) was added at 0 °C, followed by DIPEA

(0.61 mL, 3.52 mmol), and the reaction mixture was further stirred for 16 h at RT. The mixture was then concentrated and purified by flash column chromatography (SiO_2, c-hexane/EtOAc 1:0 to 0:1) to give *tert*-butyl (1*R*,3*S*,5*R*)-3-((6-(trifluoromethyl)pyridin-2-yl)carbamoyl)-2-azabicyclo[3.1.0]hexane-2-carboxylate as a white solid (578 mg, yield 88%). TLC, R_f (EtOAc) 0.85. LC−MS (ESI, *m/z*) 372.3 $[M+H]^+$, 370.2 $[M-H]^-$. t_R (HPLC, conditions d) 2.07 min (purity >99%). ^{1}H NMR (400 MHz, DMSO-d_6) δ (ppm) 10.9 (s, 1H), 8.38 (br d, J = 8.2 Hz, 1H), 8.10 (t, J = 7.9 Hz, 1H), 7.61 (d, J = 7.5 Hz, 1H), 4.20 (m, 1H), 3.43 (m, 1H), 2.33 (m, 1H), 2.15 (m, 1H), 1.61 (m, 1H), 1.42 (s, 3H), 1.25 (s, 6H), 0.76 (m, 1H), 0.41 (m, 1H).

To a solution of *tert*-butyl (1*R*,3*S*,5*R*)-3-((6-(trifluoromethyl)pyridin-2-yl)carbamoyl)-2-azabicyclo[3.1.0]hexane-2-carboxylate (550 mg, 1.26 mmol) in CH_2Cl_2 (8 mL) was added TFA (0.97 mL, 12.6 mmol) and the solution was stirred for 2 h at RT. The volatiles were then evaporated and the crude residue was dried under high vacuum to give the (1*R*,3*S*,5*R*)-*N*-(6-(trifluoromethyl)pyridin-2-yl)-2-azabicyclo[3.1.0]hexane-3-carboxamide di(trifluoroacetate) salt as a pale colored oil. The material thus obtained was stored at 4 °C to avoid decomposition and was used without further purification in the next reaction step. LC−MS (ESI, *m/z*) 272.1 $[M+H]^+$. ^{1}H NMR (400 MHz, DMSO-d_6) δ (ppm) 14.5 (s, 1H), 9.85 (br s, 1H), 9.27 (br s, 1H), 8.32 (br d, J = 8.2 Hz, 1H), 8.18 (t, J = 8.0 Hz, 1H), 7.71 (d, J = 7.6 Hz, 1H), 4.21 (m, 1H), 3.38 (m, 1H), 2.66 (dd, J = 12.8, 7.7 Hz, 1H), 2.13 (td, J = 11.8, 4.3 Hz, 1H), 1.86 (m, 1H), 0.85 (m, 2H).

(1*R*,3*S*,5*R*)-2-Azabicyclo[3.1.0]hexane-2,3-dicarboxylic acid 2-[(1-carbamoyl-1*H*-indol-3-yl)-amide] 3-[(6-trifluoromethyl-pyridin-2-yl)-amide] (**25**) was obtained as a white solid (39 mg, yield 21%) according to General Procedure 2 from (1*R*,3*S*,5*R*)-*N*-(6-(trifluoromethyl)pyridin-2-yl)-2-azabicyclo[3.1.0]hexane-3-carboxamide di(trifluoroacetate) salt. TLC, R_f (CH_2Cl_2/MeOH 95:5) 0.35. t_R (HPLC conditions c) 3.91 min (purity >99%). LC−MS (ESI, *m/z*) 473.2 $[M+H]^+$,

945.3 $[2M+H]^+$, 471.1 $[M-H]^-$, 943.3 $[2M-H]^-$. 1H NMR (400 MHz, DMSO-d6): δ (ppm) 10.8 (s, 1H), 8.66 (s, 1H), 8.37 (d, *J* = 8.6 Hz, 1H), 8.27 (d, *J* = 8.3 Hz, 1H), 8.07 (t, *J* = 8.0 Hz, 1H), 7.99 (s, 1H), 7.79 (d, *J* = 7.8 Hz, 1H), 7.59 (d, *J* = 7.5 Hz, 1H), 7.37 (br s, 2H), 7.26 (t, *J* = 7.5 Hz, 1H), 7.18 (t, *J* = 7.5 Hz, 1H), 4.39 (t, *J* = 8.0 Hz, 1H), 3.93 (m, 1H), 2.37 (dd, *J* = 12.9, 8.9 Hz, 1H), 2.16 (m, 1H), 1.80 (m, 1H), 0.84 (m, 1H), 0.54 (m, 1H). HRMS *m*/*z* (ESI) calcd for $C_{22}H_{20}O_3N_6F_3$ $[M+H]^+$ 473.15435; found, 473.15463.

(1*R*,3*S*,5*R*)-2-Aza-bicyclo[3.1.0]hexane-2,3-dicarboxylic acid 3-[(6-bromo-pyridin-2-yl)-amide] 2-[(1-carbamoyl-1*H*-indol-3-yl)-amide] (26). To a solution of ((1*R*,3*S*,5*R*)-2-aza-bicyclo[3.1.0]hexane-3-carboxylic acid (6-bromo-pyridin-2-yl)-amide di(trifluoroacetate) salt[7] (1.20 g, 3.03 mmol) and Et_3N (1.26 mL, 9.09 mmol) in THF (0.4 mL) was added a suspension of **32** (610 mg, 3.03 mmol) in THF (40 mL). The solution was stirred at RT under nitrogen for 45 min, volatiles were then evaporated and the residue was purified by prep HPLC (Waters SunFire C18-ODB; particle size 5 μm; column size 19 x 50 mm; eluent/gradient 20-100% CH_3CN/H_2O in 25 min (CH_3CN and H_2O containing 0.1% TFA); flow rate 40 mL/min). To the combined pure fractions was added a saturated $NaHCO_3$ solution, the aqueous layer was extraced with CH_2Cl_2, the organics were dried (Na_2SO_4) and volatiles were removed under reduced pressure to give, after drying in vacuo, a white solid (1.4 g, yield 78%). TLC, R_f (CH_2Cl_2/MeOH 9:1) 0.45. LC−MS (ESI, *m/z*) 483.1/485.2 $[M+H]^+$, 965.3/967.3 $[2M+H]^+$, 481.1/483.1 $[M-H]^-$. t_R (HPLC conditions c) 3.85 min (purity 99%). ^{1}H NMR (400 MHz, DMSO-d_6): δ (ppm) 10.7 (br s, 1H), 8.66 (br s, 1H), 8.28 (d, *J* = 8.3 Hz, 1H), 8.10 (d, *J* = 8.0 Hz, 1H), 8.00 (s, 1H), 7.80 (d, *J* = 7.8 Hz, 1H), 7.75 (t, *J* = 7.9 Hz, 1H), 7.38 (m, 2H), 7.35 (d, *J* = 7.6 Hz, 1H), 7.27 (t, *J* = 7.3 Hz, 1H), 7.20 (t, *J* = 7.1 Hz, 1H), 4.35 (t, *J* = 7.8 Hz, 1H), 3.93 (m, 1H), 2.38 (dd, *J* = 12.9, 8.9 Hz, 1H),

2.17 (m, 1H), 1.80 (m, 1H), 0.85 (m, 1H), 0.55 (m, 1H). HRMS *m*/*z* (ESI) calcd for $C_{21}H_{20}O_3N_6{}^{79}Br$ $[M+H]^+$ 483.07748; found, 483.07721.

3-(2-((1*R*,3*S*,5*R*)-3-((2-Fluoro-3-(trifluoromethoxy)phenyl)carbamoyl)-2-azabicyclo[3.1.0]hexan-2-yl)-2-oxoethyl)-1*H*-indole-1-carboxamide (27). To a solution of (1*R*,3*S*,5*R*)-*N*-(2-fluoro-3-(trifluoromethoxy)phenyl)-2-azabicyclo[3.1.0]hexane-3-carboxamide trifluoro acetate salt (59.3 mg, 0.14 mmol, prepared according to General Procedure 1 by starting from (1*R*,3*S*,5*R*)-2-(*tert*-butoxycarbonyl)-2-azabicyclo[3.1.0]hexane-3-carboxylic acid and 2-fluoro-3-(trifluoromethoxy)aniline [CAS 1159512-64-7] and heating the reaction mixture at 70°C in step A), (1-carbamoyl-1*H*-indol-3-yl)-acetic acid (**33**) (30 mg, 0.14 mmol) and HBTU (78 mg, 0.21 mmol) in CH_2Cl_2 (4 mL) were added under a nitrogen atmosphere DIPEA (96 µL, 0.55 mmol) and the reaction mixture was stirred at RT for 2 h. To the mixture was then added water and EtOAc, the layers were separated and the aqueous phase was back-extracted twice with EtOAc. The combined organics were dried (Na_2SO_4), filtered and concentrated. The residue was purified by prep HPLC (Waters SunFire C18-ODB; particule size 5 µm; column size 30 x 100 mm; eluent/gradient 5% CH_3CN/H_2O 2.5 min, 5-100% CH_3CN in H_2O for 10 min (CH_3CN and H_2O containing 0.1% HCOOH); flow rate 40 mL/min) to give after extraction and concentration of the pure fractions the title compound **27** as a white powder (40 mg, yield 58%). TLC, R_f (AcOEt) 0.7. LC−MS (ESI, *m/z*) 505.1 $[M+H]^+$, 522.2 $[M+18]^+$, 503.1 $[M-H]^-$. t_R (HPLC conditions a) 3.57 min (purity >99%). t_R (HPLC conditions d) 2.1 min (purity >99%). ^1H NMR (400 MHz, DMSO-d_6): δ (ppm) 9.95 (br s, 1H), 8.25 (d, *J* = 8.3 Hz, 1H), 7.89 (m, 1H), 7.78 (s, 1H), 7.58 (d, *J* = 7.8 Hz, 1H), 7.47 (br s, 2H), 7.34-7.23 (m, 3H), 7.16 (t, *J* = 7.1 Hz, 1H), 4.49 (dd, *J* = 8.2, 6.1 Hz, 1H), 3.95 (s, 2H), 3.75 (m, 1H), 2.27 (m, 2H), 1.84 (m, 1H), 0.96

(m, 1H), 0.58 (m, 1H). HRMS *m/z* (ESI) calcd for $C_{24}H_{21}O_4N_4F_4$ $[M+H]^+$ 505.14934; found, 505.14948.

1-{2-[(1*R*,3*S*,5*R*)-3-(6-Bromo-pyridin-2-ylcarbamoyl)-2-aza-bicyclo[3.1.0]hex-2-yl]-2-oxo-ethyl}-1*H*-indole-3-carboxylic acid amide (28). Beige solid (23 mg, yield 61%) prepared according to the procedure described for **27** from ((1*R*,3*S*,5*R*)-2-aza-bicyclo[3.1.0]hexane-3-carboxylic acid (6-bromo-pyridin-2-yl)-amide di(trifluoroacetate) salt[7] and 2-(3-carbamoyl-1H-indol-1-yl)acetic acid [CAS 1016689-54-5]. TLC, R_f (CH_2Cl_2/MeOH 90:10) 0.45. t_R (HPLC conditions a) 2.62 min (purity >99%). t_R (HPLC conditions d) 1.65 min (purity >99%). LC−MS (ESI, *m/z*) 482.1/484.1 $[M+H]^+$, 499.2/501.2 $[M+NH_4]^+$, 480.1/482.1 $[M-H]^-$. ^{1}H NMR (400 MHz, DMSO-d_6): δ (ppm) 10.8 (s, 1H), 8.15 (d, *J* = 7.8 Hz, 1H), 8.04 (d, *J* = 8.1 Hz, 1H), 7.98 (s, 1H), 7.72 (t, *J* = 8.0 Hz, 1H), 7.42 (d, *J* = 8.1 Hz, 1H), 7.33 (d, *J* = 7.7 Hz, 1H), 7.19 (m, 1H), 7.13 (t, *J* = 7.3 Hz, 1H), 5.48 (d, *J* = 17.3 Hz, 1H), 5.23 (d, *J* = 17.3 Hz, 1H), 4.45 (dd, *J* = 9.0, 5.4 Hz, 1H), 3.82 (m, 1H), 3.31 (s, 2H), 2.33 (m, 1H), 2.22 (m, 1H), 1.89 (m, 1H), 1.03 (m, 1H), 0.73 (m, 1H). HRMS *m/z* (ESI) calcd for $C_{22}H_{21}O_3N_5{}^{79}Br$ $[M+H]^+$ 482.08223; found, 482.08221.

(1*R*,3*S*,5*R*)-2-(2-(3-Acetyl-1*H*-indazol-1-yl)acetyl)-*N*-(6-bromopyridin-2-yl)-2-azabicyclo[3.1.0]hexane-3-carboxamide (29). White solid (30 mg, yield 79%) prepared according to the procedure described for **27** from ((1*R*,3*S*,5*R*)-2-aza-bicyclo[3.1.0]hexane-3-carboxylic acid (6-bromo-pyridin-2-yl)-amide di(trifluoroacetate) salt[7] and 2-(3-acetyl-1*H*-indazol-1-yl)acetic acid (**36**). TLC, R_f (CH_2Cl_2/MeOH 90:10) 0.9. t_R (HPLC conditions a) 3.25 min (purity >99%). t_R (HPLC conditions d) 1.85 min (purity >99%). LC−MS (ESI, *m/z*) 482.1/484.1 $[M+H]^+$, 499.1/501.2 $[M+NH_4]^+$, 963.3/965.3 $[2M+H]^+$, 980.3/982.3 $[2M+NH_4]^+$, 480.2/482.5 $[M-H]^-$, 526.1/528.0 $[M+HCOO]^-$. ^{1}H NMR (400 MHz, DMSO-d_6): δ (ppm) 10.8 (s, 1H), 8.19 (d, *J* = 8.1 Hz, 1H), 8.04 (d, *J* = 8.1 Hz, 1H), 7.72 (m, 2H), 7.50 (t, *J* = 7.7 Hz, 1H),

7.36 (m, 2H), 5.95 (d, *J* = 17.2 Hz, 1H), 5.58 (d, *J* = 17.2 Hz, 1H), 4.46 (dd, *J* = 9.0, 5.4 Hz, 1H), 3.85 (m, 1H), 3.30 (s, 2H), 2.64 (s, 3H), 2.35 (dd, *J* = 13.1, 9.6 Hz, 1H), 2.23 (m, 1H), 1.92 (m, 1H), 1.02 (m, 1H), 0.80 (m, 1H). HRMS *m*/*z* (ESI) calcd for $C_{22}H_{21}O_3N_5{}^{79}Br$ $[M+H]^+$ 482.08223; found, 482.08221.

1-(2-((1*R*,3*S*,5*R*)-3-((3-Bromo-2-fluorophenyl)carbamoyl)-2-azabicyclo[3.1.0]hexan-2-yl)-2-oxoethyl)-1*H*-indazole-3-carboxamide (30). White solid (30 mg, yield 61%) prepared according to the procedure described for **27** from (1*R*,3*S*,5*R*)-*N*-(3-bromo-2-fluorophenyl)-2-azabicyclo[3.1.0]hexane-3-carboxamide trifluoroacetate salt (prepared according to General Procedure 1 by starting from (1*R*,3*S*,5*R*)-2-(*tert*-butoxycarbonyl)-2-azabicyclo[3.1.0]hexane-3-carboxylic acid and 3-bromo-2-fluoroaniline and using CH_2Cl_2 as the solvent in step A) and 2-(3-carbamoyl-1*H*-indazol-1-yl)acetic acid (**35**).[7] TLC, R_f (AcOEt) 0.6. t_R (HPLC conditions a) 3.18 min (purity >99%). t_R (HPLC conditions d) 1.90 min (purity >99%). LC−MS (ESI, *m/z*) 517.1/519.1 $[M+NH_4]^+$, 498.1/500.1 $[M-H]^-$, 544.1/546.0 $[M+HCOO]^-$. ^{1}H NMR (400 MHz, DMSO-d_6): δ (ppm) 9.84 (s, 1H), 8.19 (d, *J* = 8.3 Hz, 1H), 7.77 (m, 1H), 7.67 (br s, 1H), 7.66 (d, *J* = 8.6 Hz, 1H), 7.48-7.43 (m, 2H), 7.39 (br s, 1H), 7.28 (t, *J* = 7.6 Hz, 1H), 7.12 (td, *J* = 8.1, 1.2 Hz, 1H), 5.81 (d, *J* = 17.4 Hz, 1H), 5.51 (d, *J* = 17.4 Hz, 1H), 4.50 (dd, *J* = 8.6, 5.4 Hz, 1H), 3.80 (m, 1H), 2.28 (m, 2H), 1.92 (m, 1H), 1.03 (m, 1H), 0.77 (m, 1H). HRMS *m*/*z* (ESI) calcd for $C_{22}H_{20}O_3N_5{}^{79}BrF$ $[M+H]^+$ 500.07281; found, 500.07271.

3-Isocyanato-1-methyl-1*H*-indole (31). To a suspension of 1-methylindole-3-carboxylic acid (**44**) ([*CAS* 32387-21-6]; 700 mg, 4.00 mmol) in toluene (21 mL) under nitrogen was added triethylamine (Et_3N; 556 μL, 4.00 mmol). After 15 min, diphenylphosphoryl azide (DPPA, 90% purity; 960 μL, 4.0 mmol) was added and the reaction mixture was further stirred at RT for 8 h to give an orange solution. TLC indicated consumption of the starting material and formation of the

acyl azide intermediate (R_f (c-hexane/EtOAc 1:1) 0.6). The mixture was concentrated under reduced pressure (Caution! Azides are potentially explosive substances and can decompose violently) and the crude residue was purified by flash column chromatography (SiO_2, c-hexane to c-hexane/EtOAc 3:2) to give the intermediate acyl azide (700 mg). ^{1}H NMR (400 MHz, DMSO-d_6): δ (ppm) 8.25 (s, 1H), 8.05 (d, J = 7.1 Hz, 1H), 7.59 (d, J = 7.6 Hz, 1H), 7.34-7.27 (m, 2H), 3.88 (s, 3H). The acyl azide intermediate (700 mg) was refluxed in toluene (20 mL) for 16 h. Toluene was evaporated under reduced pressure to give **31** as a slightly brown oil (609 mg, yield 89%) which was used without purification in the next step. TLC, R_f (c-hexane/EtOAc 1:2) 0.35. t_R (HPLC conditions a): 3.85 min (purity >90%). ^{1}H NMR (400 MHz, $CDCl_3$) δ (ppm) 7.60 (dt, J = 8.0, 0.9 Hz, 1H), 7.30 (m, 2H), 7.18 (ddd, J = 8.0, 6.3, 1.8 Hz, 1H), 6.91 (s, 1H), 3.75 (s, 3H).

3-Isocyanato-indole-1-carboxylic acid amide (32). To a solution of 1*H*-indole-3-carboxylic acid (**41**) ([*CAS* 771-50-6]; 5.0 g, 31 mmol) in DMF (70 mL) under nitrogen atmosphere, cooled to 0 °C, was added cesium carbonate (11 g, 31 mmol) and benzyl bromide (4.05 mL, 34.1 mmol). The reaction mixture was stirred at RT for 48 h and then was poured into water. EtOAc was added, the layers were separated and the aqueous phase was back-extracted three times with EtOAc. The combined organics were washed with water, dried (Na_2SO_4), filtered and concentrated. The residue was taken up in Et_2O and the resulting precipitate was filtered off to give 1*H*-indole-3-carboxylic acid benzyl ester (**42**) as a white powder (6.46 g, yield 83%). TLC, R_f (c-hexane/EtOAc 1:1) 0.55. t_R (HPLC conditions a) 3.8 min (purity >99%). LC−MS (ESI, *m/z*) 252.1 $[M+H]^+$, 274.0 $[M+Na]^+$, 525.1 $[2M+Na]^+$, 250.1 $[M-H]^-$. ^{1}H NMR (400 MHz, DMSO-d_6): δ (ppm) 12.0 (s, 1H), 8.14 (s, 1H), 7.98 (d, J = 6.8 Hz, 1H), 7.48 (m, 3H), 7.40 (m, 2H), 7.33 (m, 1H), 7.19 (m, 2H), 5.33 (s, 2H).

To a solution of **42** (3.50 g, 13.9 mmol) in tetrahydrofuran (THF; 70 mL), cooled to 5 °C under a nitrogen atmosphere, was added sodium hydride (NaH, 60% in mineral oil; 557 mg, 13.9 mmol). The mixture was stirred at 5 °C for 30 min, followed by slow dropwise addition of chlorosulfonyl isocyanate (2.42 mL, 27.9 mmol) while maintaining the temperature between 5 and 10 °C. The pale yellow solution was further stirred at RT for 3.5 h. Acetic acid (22.5 mL) was added (exothermic) and the resulting solution was stirred at RT for 1.5 h, followed by addition of ice cubes and water (100 mL). The white thick suspension was stirred at RT for 30 min. The precipitate formed was then filtered off, taken up in MeOH and filtered off again to afford 1-carbamoyl-1*H*-indole-3-carboxylic acid benzyl ester (**43**) as a white powder (1.19 g, yield 29%). LC−MS (ESI, *m/z*) 295.1 $[M+H]^+$, 317.0 $[M+Na]^+$, 611.0 $[2M+Na]^+$. ^{1}H NMR (400 MHz, DMSO-d_6): δ (ppm) 8.64 (s, 1H), 8.29 (d, J = 7.6 Hz, 1H), 8.04 (d, J = 7.35 Hz, 1H), 7.90 (m, 2H), 7.50 (m, 2H), 7.42 (m, 2H), 7.36-7.30 (m, 3H), 5.38 (s, 2H).

To a solution of **43** (1.33 g, 4.52 mmol) in a mixture of DMF/THF 1:1 (28 mL) was added Pd/10% C (250 mg) and the solution was degassed three times by replacing air with nitrogen and then nitrogen by hydrogen gas. The reaction mixture was stirred overnight, and the catalyst was then removed by filtration through a pad of Celite followed by washing with THF. The solvents were concentrated under high vacuum to give a yellowish solid which was taken up in Et_2O and filtered off to afford 1-carbamoyl-1*H*-indole-3-carboxylic acid (**45**) as a solid (900 mg, yield 100%). TLC, R_f (CH_2Cl_2/MeOH 9:1) 0.25. LC−MS (ESI, *m/z*) 205.1 $[M+H]^+$, 249.1 $[M+HCOO]^-$. ^{1}H NMR (400 MHz, DMSO-d_6): δ (ppm) 12.6 (m, 1H), 8.55 (s, 1H), 8.29 (d, J = 7.85 Hz, 1H), 8.06 (d, J = 7.35 Hz, 1H), 7.85 (m, 2H), 7.34-7.27 (m, 2H).

To a white suspension of **45** (6.00 g, 29.4 mmol) in CH_2Cl_2[36] (80 mL) under nitrogen was added Et_3N (4.50 mL, 32.3 mmol) at 12-18 °C. After stirring for 1 h at -15 °C, DPPA (7.0 mL, 32.3

mmol) was added over 10 min to the colorless solution and the reaction mixture was stirred at 15 °C for 7 h. The white suspension was filtered off and the precipitate was washed with cold CH_2Cl_2 (10 mL) to give the intermediate acyl azide. The wet cake was stored under an argon atmosphere at -30 °C and used without purification in the following reaction step (**Warning!** The acyl azide intermediate has a relatively low onset temperature of decomposition with a large energy release (dynamic DSC: onset T = 139.6 °C, 963 J/g). ^{1}H NMR (400 MHz, DMSO-d_6): δ (ppm) 8.70 (s, 1H), 8.30 (d, J = 7.35 Hz, 1H), 8.11 (d, J = 6.50 Hz, 1H), 8.04 (m, 2H), 7.38 (m, 2H). The wet acyl azide intermediate was added portionwise (about 1 g to 1.5 g as white suspension in toluene (5 mL) every 1.5 h) to toluene (125 mL) heated at 100-105 °C. Five min after the addition of one portion of the acyl azide suspension, the reaction mixture became colorless and HPLC after 30 min indicated disappearance of the azide. This procedure was repeated until full consumption of the azide was accomplished. The reaction mixture was allowed to warm to RT, the yellow suspension was filtered and the filtrate was concentrated under reduced pressure to give 3-isocyanato-indole-1-carboxylic acid amide (**32**) as a white powder (3.06 g, yield 52%) which was stored at 4 °C under an argon atmosphere before use without further purification in the next reaction step. ^{1}H NMR (400 MHz, $CDCl_3$): δ (ppm) 8.19 (d, J = 8.4 Hz, 1H), 7.62 (d, J = 7.8 Hz, 1H), 7.44 (m, 1H), 7.35 (m, 1H), 7.26 (s, 1H), 5.39 (m, 2H).

(1-Carbamoyl-1*H*-indol-3-yl)-acetic acid (33). To a solution of (1*H*-indol-3-yl)-acetic acid ethyl ester (**46**) ([*CAS* 778-82-5]; 2.50 g, 12.3 mmol) in THF (58 mL), cooled to 0 °C, was added NaH (60% in mineral oil; 0.354 g, 14.8 mmol) portionwise under an argon atmosphere. The dark brown solution was stirred at 0 °C for 45 min, followed by dropwise addition of chlorosulfonylisocyanate (CSI; 2.14 mL, 24.6 mmol). The reaction mixture was allowed to warm

to RT overnight with stirring. Acetic acid (3 mL) was then added to the mixture which was stirred at RT for another 20 min. Wet ice was added and the mixture was further stirred for 60 min, then diluted with water and extracted three times with EtOAc. The combined organics were washed with brine, dried (phase separator) and concentrated in vacuo. The residual oil was purified by flash column chromatography (SiO_2, c-hexane/EtOAc 3:1 to 3:2) to give (1-carbamoyl-1*H*-indol-3-yl)-acetic acid ethyl ester (**47**) as a brownish solid (2.0 g, yield 75%). TLC, R_f (c-hexane/EtOAc 1:1) 0.35. LC−MS (ESI, *m/z*) 247 $[M+H]^+$, 493 $[2M+H]^+$. t_R (HPLC conditions b) 3.51 min. ^{1}H NMR (400 MHz, DMSO-d_6): δ (ppm) 8.24 (d, J = 8.35 Hz, 1H), 7.76 (s, 1H), 7.54 (d, J = 7.85 Hz, 1H), 7.52 (br s, 2H), 7.25 (t, J = 7.7 Hz, 1H), 7.17 (t, J = 7.5 Hz, 1H), 4.10 (q, J = 7.1 Hz, 2H), 3.75 (s, 2H), 1.19 (t, J = 7.1 Hz, 3H).

To a suspension of **47** (2.00 g, 6.09 mmol) in MeOH (61 mL) and water (6.1 mL) was added a 1 N aqueous solution of NaOH (12.2 mL, 12.2 mmol) and the resulting yellow solution was stirred at RT for 4 h. The reaction mixture was concentrated under reduced pressure and the residue was suspended in aqueous 1 N HCl. The aqueous layer was extracted with EtOAc (3x), the combined organics were dried (phase separator) and concentrated in vacuo to afford the crude product **33** as a brownish solid (1.02 g, yield 95%), which was used directly in the next step. LC−MS (ESI, *m/z*) 219 $[M+H]^+$, 437 $[2M+H]^+$. t_R (HPLC conditions b) 2.16 min. ^{1}H NMR (400 MHz, DMSO-d_6): δ (ppm) 8.23 (d, J = 8.2 Hz, 1H), 7.74 (s, 1H), 7.53 (d, J = 7.7 Hz, 1H), 7.50 (br s, 2H), 7.24 (t, J = 7.6 Hz, 1H), 7.17 (t, J = 7.5 Hz, 1H), 3.64 (s, 2H).

2-(3-Acetyl)-1*H*-indazol-1-yl)acetic acid (36). To a solution of 1-(1*H*-indazol-3-yl)ethanone (**48**) ([*CAS* 4498-72-0]; 2.00 g, 12.5 mmol) in acetonitrile (50 mL) was added K_2CO_3 (3.97 g, 28.7 mmol) and *tert*-butyl 2-bromoacetate (3.41 g, 17.5 mmol). The reaction mixture was stirred for 18 h at reflux temperature. After cooling to RT, the mixture was filtered, and the filtrate was

evaporated under reduced pressure to afford crude *tert*-butyl 2-(3-acetyl-1*H*-indazol-1-yl)acetate (**49**) as a yellow oil. LC−MS (ESI, *m/z*) 275 $[M+H]^+$. t_R (HPLC conditions e) 5.04 min. ^{1}H NMR (400 MHz, DMSO-d_6): δ (ppm) 8.21 (d, J = 8.1 Hz, 1H), 7.76 (d, J = 8.5 Hz, 1H), 7.52 (t, J = 7.9 Hz, 1H), 7.38 (t, J = 7.5 Hz, 1H), 5.46 (s, 2H), 2.64 (s, 3H), 1.43 (s, 9H).

To a solution of **49** (12.5 mmol) in CH_2Cl_2 (45 mL) was added TFA (15 mL, 14.4 mmol) and stirring was continued at RT overnight. The reaction mixture was evaporated, the residue was taken up in MeOH and volatiles were removed again under reduced pressure to afford **36** as a yellowish solid (2.97 g, yield 100% over two reaction steps). The material thus obtained was used directly in the next step without further purification. LC−MS (ESI, *m/z*) 219.1 $[M+H]^+$, 217.1 $[M-H]^-$. t_R (HPLC conditions e) 3.48 min (purity 95%). ^{1}H NMR (400 MHz, DMSO-d_6): δ (ppm) 13.3 (br s, 1H), 8.21 (d, J = 8.1 Hz, 1H), 7.79 (d, J = 8.5 Hz, 1H), 7.51 (t, J = 7.7 Hz, 1H), 7.38 (t, J = 7.5 Hz, 1H), 5.46 (s, 2H), 2.64 (s, 3H).

(2*S*,4*R*)- and **(2*S*,4*S*)-2-(3-Trifluoromethoxy-phenylcarbamoyl)-4-methyl-pyrrolidine-1-carboxylic acid *tert*-butyl ester (39** and **40).** To a suspension of *N*-Boc-4-methylene-L-proline (**37**) ([*CAS*84348-38-9]; 1.00 g, 4.40 mmol) in CH_2Cl_2 (40 mL) was added 3-(trifluoromethoxy)aniline (0.71 mL, 5.28 mmol), HBTU (1.14 g, 6.60 mmol) and DIPEA (1.51 mL, 8.80 mmol). The reaction mixture was stirred at RT for 2 days under a nitrogen atmosphere, and then was successively washed with 30 mL of a saturated aqueous $NaHCO_3$ solution and aqueous 1 N HCl. The organic layers were dried (phase separator) and concentrated under vacuum. The crude residue was purified by flash column chromatography (SiO_2, c-hexane/EtOAc 65:35) to afford (*S*)-2-(3-trifluoromethoxy-phenylcarbamoyl)-4-methylene-pyrrolidine-1-carboxylic acid *tert*-butyl ester (**38**) as a yellow oil (1.7 g, yield 100%). TLC, R_f (c-hexane/EtOAc 1:1) 0.55. LC−MS (ESI, *m/z*) 287.0 $[M-Boc]^+$, 385.0 $[M-H]^-$. ^{1}H NMR (400

MHz, DMSO-d_6): δ (ppm) 10.4 (s, 1H), 7.77 (s, 1H), 7.50-7.42 (m, 2H), 7.04 (br d, J = 7.8 Hz, 1H), 5.00 (m, 2H), 4.41 (m, 1H), 4.06-3.94 (m, 2H), 3.01 (m, 1H), 2.58 (m, 1H), 1.40 (s, 4H), 1.28 (s, 5H).

To a solution of **38** (0.50 g, 1.29 mmol) in EtOAc (15 mL) was added Pd/C (10 %) (50 mg) and the solution was degassed three times by replacing air with nitrogen and then nitrogen with hydrogen gas. The reaction mixture was stirred at RT overnight, then was filtered over a pad of Celite followed by washing the residual catalyst with EtOAc and the evaporation of solvents. The crude material was purified by prep HPLC (Waters SunFire C18-ODB; particle size 5 µm; column size 30 x 100 mm; eluent/gradient 20-100% CH_3CN in H_2O for 20 min, 100% CH_3CN/2 min (CH_3CN and H_2O containing 0.1% TFA); flow rate 40 mL/min; loading 150 mg per run) to afford after lyophilization of the corresponding fractions the two title compounds as pure diastereoisomers: (2*S*,4*S*)-2-(3-trifluoromethoxy-phenylcarbamoyl)-4-methyl-pyrrolidine-1-carboxylic acid *tert*-butyl ester (**40**) as a white foam (270 mg, yield 53%). t_R (HPLC, conditions b) 5.34 min. LC−MS (ESI, *m/z*) 387.0 $[M-H]^-$. ^{1}H NMR (400 MHz, DMSO-d_6): δ (ppm): 10.3 (s, 1H), 7.80 (m, 1H), 7.53 (d, J = 8.1 Hz, 1H), 7.45 (t, J = 8.2 Hz, 1H), 7.04 (br d, J = 8.1 Hz, 1H), 4.19 (m, 1H, H_2), 3.62 (m, 1H, H_5), 2.87 (m, 1H, H_5), 2.35 (m, 1H, H_3), 2.22 (m, 1H, H_4), 1.47 (m, 1H, H_3), 1.39 (s, 3H), 1.34 (s, 6H), 1.03 (d, J = 6.6 Hz, 3H); the ROESY NMR spectrum showed nOe effects between H_2 and H_4 in line with absolute (2*S*,4*S*)-configuration. (2*S*,4*R*)-2-(3-trifluoromethoxy-phenylcarbamoyl)-4-methyl-pyrrolidine-1-carboxylic acid *tert*-butyl ester (**39**) as a white foam (35 mg, yield 7%): t_R (HPLC, conditions b) 5.53 min. LC−MS (ESI, *m/z*) 387.0 $[M-H]^-$. ^{1}H NMR (400 MHz, DMSO-d_6): δ (ppm): 10.3 (m, 1H), 7.80 (s, 1H), 7.51 (d, J = 8.5 Hz, 1H), 7.45 (t, J = 8.2 Hz, 1H), 7.05 (br d, J = 8.1 Hz, 1H), 4.28 (m, 1H, H_2), 3.61 (m, 1H, H_5), 2.89 (m, 1H, H_5), 2.38 (m, 1H, H_4), 2.02 (m, 1H, H_3), 1.86 (m, 1H, H_3), 1.41 (s, 4H), 1.27 (s,

5H), 1.00 (d, J = 6.6 Hz, 3H); the ROESY NMR spectrum showed nOe effects between H_2 and the methyl substituent, indicating absolute (2*S*,4*R*)-configuration.

Cynomolgus monkey ex vivo complement activation

Animal studies were conducted in accordance with Novartis Animal Care and Use Committee-approved protocols, and in line with facility Standard Operating Procedures (SOPs). Inhibitor **2** was formulated in 0.5% (w/v) Tween 80 in water and administered by oral gavage at 10 mg/kg or 50 mg/kg to male cynomolgus monkeys, 2 to 4 years of age, weighing 1.8 to 4 kg. Blood samples were collected once during the pre-test period (baseline sample). Additional samples were taken at the 4, 7, and 24 h time points after dosing. The serum collection tubes were allowed to clot at room temperature for at least 30 min, then centrifuged and the serum samples were obtained. Serum was diluted 50% into GVB buffer (Boston Bioproducts) containing 4 mM $MgCl_2$ and 20 mM EGTA (the final concentrations were 2 mM and 10 mM, respectively). ELISA plates (black Maxisorp™, NUNC) were coated with 1 mg/mL zymosan A (Sigma) in carbonate buffer pH 9.5 (Sigma). Serum-buffer mixture was transferred to the plate and incubated at 37 °C for 30 min. MAC complex deposited on the plate was detected by one hour incubation with an alkaline phosphatase-conjugated mouse anti-human C9 neo-epitope monoclonal antibody (clone AE11, Diatec; 0.25 μg/ml). After washing, substrate 4-MUP (Fisher) at 0.18 mg/mL in 0.1 M Tris–HCl (pH 9.0) containing 2 mM $MgCl_2$ was added and the plate was incubated for 30 min. Plates were read at 355 nm excitation/460 nm emission wavelengths on a suitable fluorometer. The raw data obtained (in relative fluorescence units, RFU) were exported into GraphPad Prism. The negative control signal (serum plus 25 mM EDTA for complete complement inhibition) was subtracted from all samples for each individual. MAC deposition in each individual animal's baseline sample was considered to be 100%

complement activity for that individual. The MAC deposition in each treated sample from the same individual was determined. % ex vivo AP activity was calculated as (baseline RFU – post-treatment RFU) *100. Alternatively, % inhibition of ex vivo MAC deposition was calculated as [(baseline RFU– post-treatment RFU)/ (baseline RFU)] * 100.

ASSOCIATED CONTENT

Supporting Information

The Supporting Information is available free of charge on the ACS Publication website at DOI:. Crystallographic structure determination of FD in complex with compounds **5**, **7**, **13**, **14**, **18** and **2**, Complement FD thioesterolysis assay, Membrane attack complex formation assay in 50% human whole blood or in 50% human or cynomolgus monkey serum, *in vivo* studies in LPS-induced AP activation in mice expressing human FD, pharmacokinetic studies for **7**: Sprague-Dawley rat pharmacokinetic study and ocular PK in Brown Norway rats.

Accession Codes

Atomic coordinates and structure factors for the crystal structures of complement Factor D with compounds **5**, **7**, **13**, **14**, **18** and **2** can be accessed using PDB codes, 5NAT, 5NAR, 5NAW, 5NBA, 5NB6, 5NB7 respectively. Authors will release the atomic coordinates and experimental data upon article publication.

AUTHOR INFORMATION

Corresponding Authors

*Corresponding Authors: To whom correspondence should be addressed: (E.L.) Tel: +41-61-6961955, E-mail: edwige.lorthiois@novartis.com; (J.M.) Tel:+41-61-6965560, E-mail: juergen_klaus.maibaum@novartis.com

Present Addresses

†Stefan Randl: Evonik Japan Co., Ltd., Shinjuku Monolith 12F, 2-3-1, Nishi-Shinjuku, Shinjuku-ku, 163-0938 Tokyo. ††Aengus Mac Sweeney: Drug Discovery Department, Actelion Pharmaceuticals Ltd., CH-4123 Allschwil, Switzerland.

Funding Sources

None.

Notes

The authors declare no competing financial interest.

ACKNOWLEDGMENT

The authors would like to thank Frederic Villard, Corinne Durand, Fabien Tritsch, Mickael Sorge, Celine Dentel, Wendy Lee, Ann Brown and Jaimie Spear for for their excellent technical assistance, Heiner Schutz for preparation of larger quantities of the isocyanate intermediate, Nathalie Gradoux for IC_{50} determinations, Susanne Glowienke and Wilfried Frieauff for performing the Ames and MNT assays, respectively. R. Sedrani is thanked for continuing helpful discussion.

ABBREVIATIONS

AP alternative pathway; FB Factor B; FD Factor D; FBS fragment based screening; MAC membrane attack complex; AMD age-related macular degeneration.

REFERENCES

1. Ricklin, D; Hajishengallis, G.; Yang, K.; Lambris, J. D. Complement: a key system for immune surveillance and homeostasis. *Nat. Immunol.* **2010**, *11*, 785–797.

2. Zarkadis, I. K.; Mastellos, D.; Lambris, J. D. Phylogenetic aspects of the complement system. *Dev. Comp. Immunol.* **2001**, *25*, 745–762.

3. Ricklin, D; Lambris, J. D. Complement-targeted therapeutics. *Nat. Biotechnol.* **2007**, *25*, 1265-1275.

4. (a) Volanakis, J. E.; Narayana, S. V. L. Complement factor D, a novel serine protease. *Protein Sci.* **1996**, *5*, 553–564; (b) Hua Jing, H.; Babu, Y. S.; Moore, D.; Kilpatrick, J. M.; Liu, X.-Y.; Volanakis, J. E.; Narayana, S. V. L. Structures of native and complexed complement factor D: Implications of the atypical His57 conformation and self-inhibitory loop in the regulation of specific serine protease activity. *J. Mol. Biol.* **1998**, *282*, 1061–1081; (c) Jing, H.; Macon, K. J.; Moore, D.; DeLucas, L. J.; Volanakis, J. E.; Narayana, S. V. L. Structural basis of profactor D activation: from a highly flexible zymogen to a novel self-inhibited serine protease, complement factor D. *EMBO J.* **1999**, *18*, 804–814.

5. Taylor, F. R.; Bixler, S. A.; Budman, J. I.; Wen, D.; Karpusas, M.; Ryan, S. T.; Jaworski, G. J.; Safari-Fard, A.; Pollard, S.; Whitty, A. Induced fit activation mechanism of the exceptionally specific serine protease, Complement Factor D. *Biochemistry* **1999**, *38*, 2849–2859.

6. Forneris, F.; Ricklin, D.; Wu, J.; Tzekou, A.; Wallace, R. S.; Lambris, J. D.; Gros P. Structures of C3b in complex with factors B and D give insight into complement convertase formation. *Science* **2010**, *330*, 1816–1820.

7. Maibaum, J.; Liao, S.-M.; Vulpetti, A.; Ostermann, N.; Randl, S.; Rudisser, S.; Lorthiois, E.; Erbel, P.; Kinzel, B.; Kolb, F. A.; Barbieri, S.; Wagner, J.; Durand, C.; Fettis, K.; Dussauge, S.; Hughes, N.; Delgado, O.; Hommel, U.; Gould, T.; Mac Sweeney, A.; Gerhartz, B.; Cumin, F.; Flohr, S.; Schubart, A.; Jaffee, B.; Harrison, R.; Risitano, A. M.; Eder, J.; Anderson, K. Small-molecule factor D inhibitors targeting the alternative complement pathway. *Nat. Chem. Biol.* **2016**, *12*, 1105–1110.

8. Vulpetti, A.; Randl, S.; Rüdisser, S.; Ostermann, N.; Erbel, P.; Mac Sweeney, A.; Zoller, T.; Salem, B.; Gerhartz, B.; Cumin, F.; Hommel, U.; Dalvit, C.; Lorthiois, E.; Maibaum, J. Structure-based library design and fragment screening for the identification of reversible complement Factor D protease inhibitors. *J. Med. Chem*. **2017**, 60, 1946–1958.

9. Morikis, D.; Lambris, J. D. Structural aspects and design of low-molecular-mass complement inhibitors. *Biochem. Soc. Trans.* **2002**, *30*, 1026–1036 and references cited therein.

10. Katschke, K. J., Jr.; Wu, P.; Ganesan, R.; Kelley, R. F.; Mathieu, M. A.; Hass, P. E.; Murray, J.; Kirchhofer, D.; Wiesmann, C.; van Lookeren Campagne, M. Inhibiting alternative pathway complement activation by targeting the factor D exosite. *J. Biol. Chem.* **2012**, *287*, 12886−12892.

11. Mastellos, D.C.; Yancopoulou, D.; Kokkinos, P.; Huber-Lang, M.; Hajishengallis, G.; Biglarnia, A.R.; Lupu,F.; Nilsson, B.; Risitano, A.M.; Ricklin, D.; Lambris, J.D. Compstatin: a

C3-targeted complement inhibitor reaching its prime for bedside intervention. *Eur. J. Clin. Invest.* **2015**, *45*, 423−440.

12. Yuan, X.; Gavriilaki, E.; Baines, A. C.; Thanassi, J. A.; Yang, G.; Podos, S. D.; Huang, Y.; Huang, M.; Brodsky, R. A. Small-molecule Factor D inhibitors selectively block the alternative pathway of complement in paroxysmal nocturnal hemoglobinuria and atypical hemolytic uremic syndrome. *Haematologica* 2**017**, *102*, 466–475.

13. Kuntz, I. D.; Chen, K.; Sharp, K. A.; Kollman, P. A. The maximal affinity of ligands. *Proc. Natl. Acad. Sci. U.S.A.* **1999**, *96*, 9997–10002.

14. Hopkins, A. L.; Groom, C. R.; Alex, A. Ligand efficiency: a useful metric for lead selection. *Drug Discovery Today* **2004**, *9*, 430–431.

15. Abad-Zapatero, C.; Metz, J. T. Ligand efficiency indices as guideposts for drug discovery. *Drug Discovery Today* **2005**, *10*, 464–469.

16. Reynolds, C. H.; Bembenek, S. D.; Tounge, B. A. The role of molecular size in ligand efficiency. *Bioorg. Med. Chem. Lett.* **2007**, *17*, 4258–4261.

17. Leeson; P. D., Springthorpe; B. The influence of drug like concepts on decision-making in medicinal chemistry. *Nat. Rev. Drug Discovery* **2007**, *6*, 881–890.

18. Perola, E. An analysis of binding efficiencies of drugs and their leads in successful drug discovery programs. *J. Med. Chem.* **2010**, *53*, 2986–2997.

19. Ryckmans, T.; Edwards, M. P.; Horne, V. A.; Correia, A. M.; Owen, D. R.; Thompson, L. R.; Tran, I.; Tutt, M. F.; Young, T. Rapid assessment of a novel series of selective CB2 agonists

using parallel synthesis protocols: a lipophilic efficiency (LipE) analysis. *Bioorg. Med. Chem. Lett.* **2009**, *19*, 4406–4409.

20. Schultz, M. D. The thermodynamic basis for the use of lipophilic efficiency in enthalpic optimization. *Bioorg. Med. Chem. Lett.* **2013**, *23*, 5992–6000.

21. Escobar, P. A.; Kemper, R. A.; Tarca, J.; Nicolette, J.; Kenyon, M.; Glowienke, S.; Sawant, S. G.; Christensen, J.; Johnson, T. E.; McKnight, C.; Ward, G.; Galloway, S.M.; Custer, L.; Gocke, E.; O'Donovan, M.R.; Braun, K.; Snyder, R. D.; Mahadevan, B. Bacterial mutagenicity screening in the pharmaceutical industry. *Mutat. Res.* **2013**, *752*, 99–118.

22. Frieauff, W.; Martus, H. J.; Suter, W.; Elhajouji, A. Automatic analysis of the micronucleus test in primary human lymphocytes using image analysis. *Mutagenesis* **2013**, *28*,15–23.

23. Gillis, E. P.; Eastman, K. J.; Hill, M. D.; Donnelly, D. J.; Meanwell, N. A. Applications of fluorine in medicinal chemistry. *J. Med. Chem.* **2015**, *58*, 8315–8359 and references cited therein.

24. Böhm, H-J.; Banner, D.; Bendels, S.; Kansy, M.; Kuhn, B.; Müller, K.; Obst-Sander, U.; Stahl, M. Fluorine in medicinal chemistry. *ChemBioChem* **2004**, *5*, 637–643.

25. Müller, K.; Faeh, C.; Diederich, F. Fluorine in pharmaceuticals: looking beyond intuition. *Science* **2007**, *317*, 1881–1886.

26. Xing, L.; Blakemore, D. C.; Narayanan, A.; Unwalla, R.; Lovering, F.; Denny, R. A.; Zhou, H.; Bunnage, M. E. Fluorine in drug design: A case study with fluoroanisoles. *ChemMedChem* **2015**, *10*, 715–726.

27. Auffinger, P.; Hays, F. A.; Westhof, E.; Ho, P. S. Halogen bonds in biological molecules. *Proc. Natl. Acad. Sci. U.S.A.* **2004**, *101*, 16789–16794.

28. Voth, A. R.; Khuu, P.; Oishi, K; Ho, P. S. Halogen bonds as orthogonal molecular interactions to hydrogen bonds. *Nat. Chem.* **2009**, *1*, 74–79.

29. Wilcken, R.; Zimmermann, M. O.; Lange, A.; Joerger, A. C.; Boeckler, F. M. Principles and applications of halogen bonding in medicinal chemistry and chemical biology. *J. Med. Chem.* **2013**, *56*, 1363−1388.

30. Parisini, E.; Metrangolo, P.; Pilati, T.; Resnati, G.; Terraneo, G. Halogen bonding in halocarbon−protein complexes: a structural survey. *Chem. Soc. Rev.* **2011**, *40*, 2267−2278.

31. Dalvit, C.; Vulpetti, A. Intermolecular and intramolecular hydrogen bonds involving fluorine atoms: Implications for recognition, selectivity, and chemical properties. *ChemMedChem* **2012**, *7*, 262–272.

32. (a) Riley, K. E.; Murray, J. S.; Fanfrlik, J.; Rezac, J.; Sola, R. J.; Concha, M. C.; Ramos, F. M.; Politzer, P. Halogen bond tunability I: the effects of aromatic fluorine substitution on the strengths of halogen-bonding interactions involving chlorine, bromine, and iodine. *J. Mol. Model.* **2011**, *17*, 3309−3318. (b) Riley, K. E.; Murray, J. S.; Fanfrlik, J.; Rezac, J.; Sola, R. J.; Concha, M. C.; Ramos, F. M.; Politzer, P. Halogen bond tunability II: the varying roles of electrostatic and dispersion contributions to attraction in halogen bonds. *J. Mol. Model.* **2013**, *19*, 4651–4659. (c) Riley, K. E.; Hobza, P. Strength and character of halogen bonds in protein−ligand complexes. *Cryst. Growth Des.* **2011**, *11*, 4272−4278.

33. Yang, C-Y.; Phillips, J. G.; Stuckey, J. A.; Bai, L.; Sun, H.; Delproposto, J.; Brown, W. C.; Chinnaswamy, K. Buried hydrogen bond interactions contribute to the high potency of complement factor D inhibitors. *ACS Med. Chem. Lett.* **2016**, *7*, 1092–1096.

34. The crystal complex structure of a structurally related compound, the preparation of which had been directly inspired by our work (WO2012093101), bound to recombinant human FD at very low 3.15 Å resolution (PDB code: 5TCA) has been reported recently (see reference 33).

35. Gleeson, M. P. Generation of a set of simple, interpretable ADMET rules of thumb. *J. Med. Chem.* **2008**, *51*, 817–834.

36. Conrow, R. E.; Dean, W. D. Diazidomethane explosion. *Org. Process Res. Dev.* **2008**, *12*, 1285–1286.

37. Warning! The acyl azide intermediate has a relatively low onset temperature of decomposition with a large energy release (dynamic DSC: onset T = 139.6 °C, 963 J/g).

38. Schramm, E. C.; Clark, S. J.; Triebwasser, M. P.; Clark, S. J.; Raychaudhuri, S.; Seddon, J. M.; Atkinson, J. P. Genetic variants in the complement system predisposing to age-related macular degeneration: a review. *Mol. Immunol.* **2014**, *61*, 118–125.

Table of Contents graphic

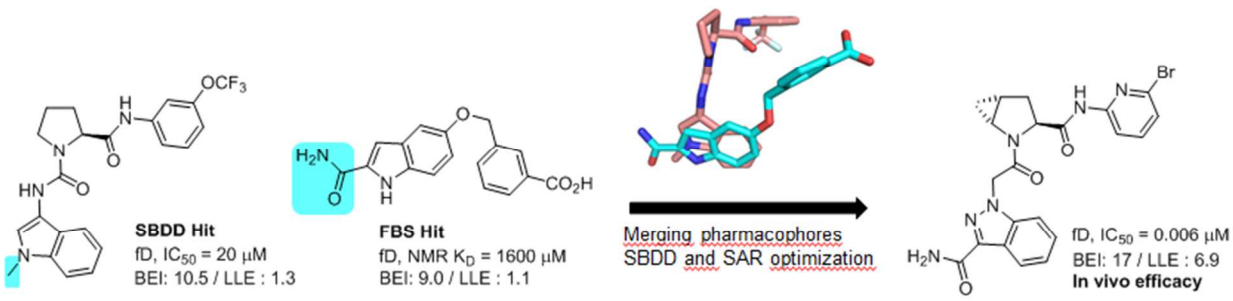
OCF3
HN
SBDD Hit
fD, IC50 = 20 μM
BEI: 10.5 / LLE : 1.3
H2N
CO2H
FBS Hit
fD, NMR KD = 1600 μM
BEI: 9.0 / LLE : 1.1
Merging pharmacophores
SBDD and SAR optimization
Br
H2N
fD, IC50 = 0.006 μM
BEI: 17 / LLE : 6.9
In vivo efficacy

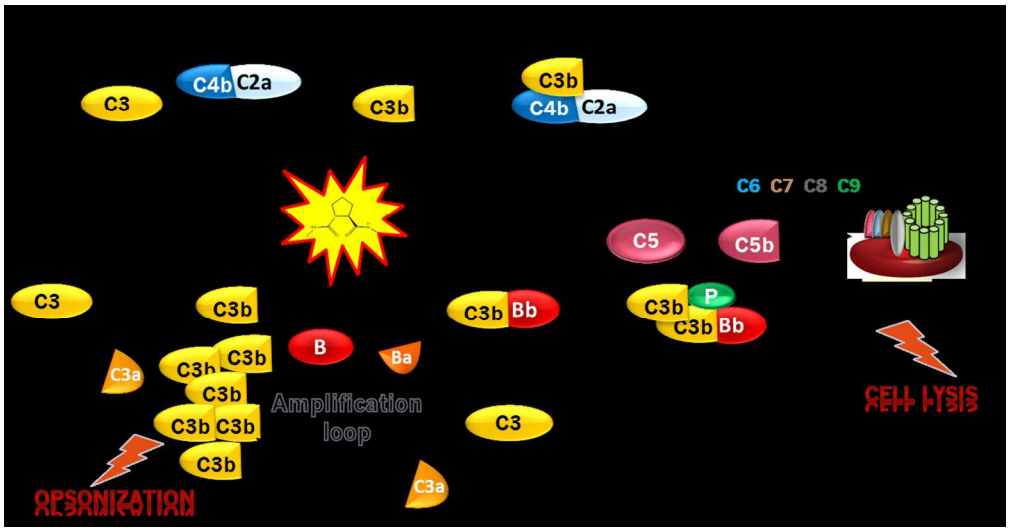

Figure 1: Schematic drawing of the classical, the lectin and the alternative complement pathways, highlighting the pivotal role of the S1 serine protease Factor D. An inhibitor of Factor D has the potential to block the initiating step of the alternative pathway (AP) and the amplification loop that augments the other two pathways, and prevent the formation of the AP C3 and C5 convertases. The key effector mechanisms of innate immunity contributed by complement are opsonization by C3 fragments and lysis by deposition of the membrane attack complex (MAC) on cell surfaces.

237x123mm (150 x 150 DPI)

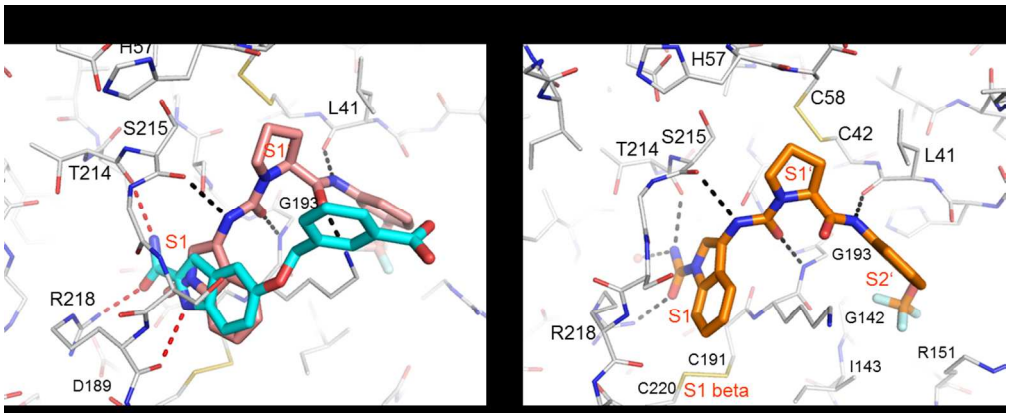

Figure 2/ Figure 2. A. Crystal structure of the complex between human FD and 5 (in pink) (PDB code: 5NAT) overlaid with FD-bound 6 (in cyan) (PDB code: 5FBI). Hydrogen-bond interactions of the urea carbonyl to the Gly193 NH (oxyanion hole) and the amide NH of compound 5 to the backbone carbonyl of Leu41 are highlighted, as well as the H-bonds of the terminal carboxamide of 6 to Thr214 of the self-inhibitory loop and to Arg218 at the bottom of the S1 pocket, and the H-bond of the indole-NH with the Arg218 backbone carbonyl. Note that the benzoic acid portion of 6 is positioned in solvent space, and hence is not resolved in the crystal structure. B. Crystal structure of the complex between human FD and 7 (in orange) (PDB code: 5NAR). The imidazole side chain of the catalytic His57 is in an ”out” conformation. The network of H-bonds between the N-carbamoyl residue of 7 and Thr214, Arg218 and a water molecule bound deeply in the S1 pocket is highlighted.

221x90mm (150 x 150 DPI)

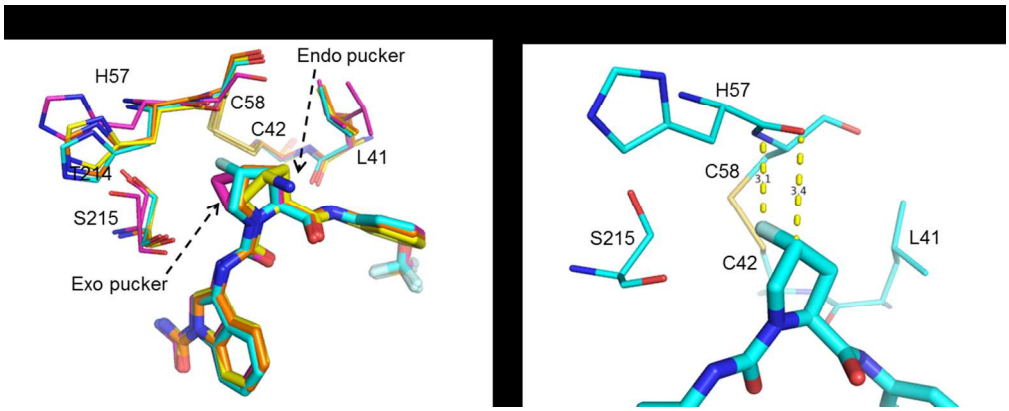

Figure 3.A. Superpositions of compounds 7 (in orange color), 13 (magenta) (PDB code: 5NAW), 14 (cyan) (PDB code: 5NBA) and 18 (yellow) (PDB code: 5NB6) observed in their X-ray crystal structures in complex to human FD. The conformational flexibility of the His57 and Ser215 side chains are highlighted, while the Cys42-Cys58 disulfide bridge conformation is largely conserved. B. Close-up view highlighting the anti-parallel dipole-dipole interaction observed between the C-F dipole in 14 and the FD His57 carbonyl dipole.

221x88mm (150 x 150 DPI)

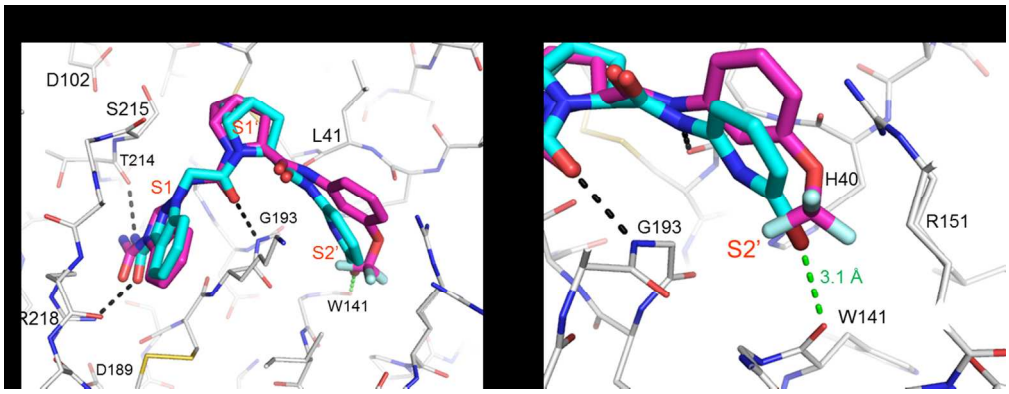

Figure 4. A. Crystal structures of human FD in complex with 2 (the protein is shown in grey color and the ligand in cyan color) (PDB code: 5NB7) overlaid with the crystal structure of the complex with compound 13 (only the ligand is shown, magenta color). The network of H-bonds (black dashed lines) in the S1 pocket, to the backbone of Gly193 and the H-bond between the amide spacer and Leu41 backbone carbonyl are conserved. B. Close up view of the S2' region, the halogen bond (green dashed lines) between the bromine atom in compound 2 and the Trp141 backbone carbonyl is highlighted.

232x88mm (150 x 150 DPI)

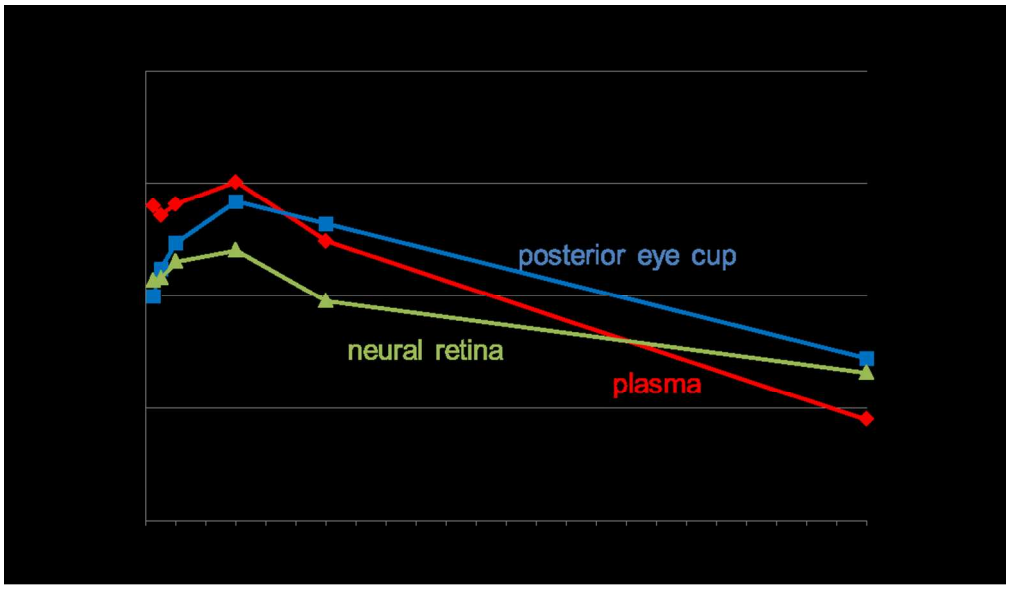

Figure 5. Plasma and ocular pharmacokinetics profiles of inhibitor 2 in Brown Norway rats after oral administration (10 mg/kg). The compound was formulated as a suspension in 0.5% HPMC and 0.1% Tween 80 and was administered by oral gavage to male 250 g Brown Norway rats (n = 2 per time point). Tissues from 2 animals were collected at 0.25, 0.5, 1, 3, 6 and 24 hours, respectively, for analysis (4 eyes/time point; each eye dissected into neural retina and posterior eye cup). Two plasma samples per time point were collected. Points represent the mean, and error bars represent the standard deviation.

197x114mm (150 x 150 DPI)

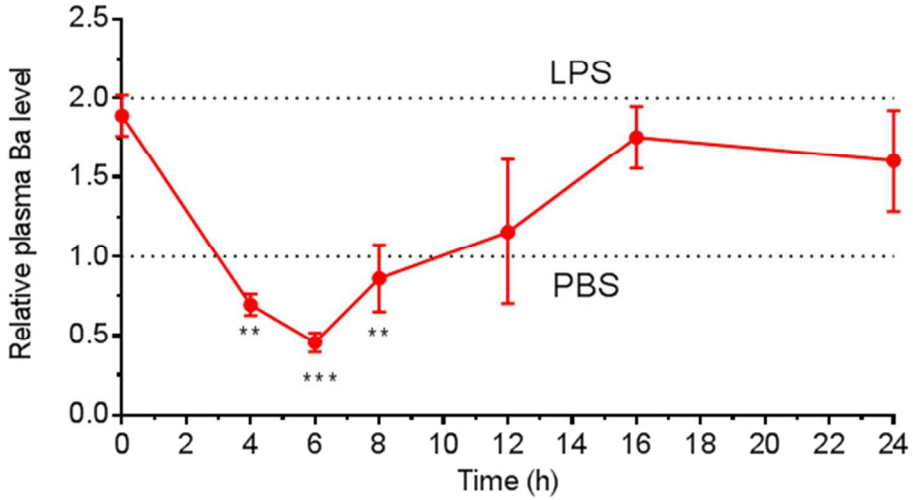

Figure 6/A: Inhibitor 2 tested at 30 mg/kg in the human factor D knock-in mouse pharmacodynamic model: (A) inhibition of Ba generation in plasma and (B) inhibition of iC3b and C3d generation in ocular tissues. Groups of mice (n = 4, female human FD knock-in) were treated either with 2 or dosing vehicle by oral gavage at 24, 16, 12, 8, 6, and 4 hours, respectively, prior to the termination of the study. All animals were given intraperitoneal LPS to activate complement 7.5 hours prior to study termination. Baseline complement levels were obtained from mice that received oral dosing vehicle and intraperitoneal saline (indicated by PBS line on graph). The positive control group received oral dosing vehicle and intraperitoneal LPS (LPS line on graph). Data shown represent mean ± s.e.m. for the group. Statistical analysis was by ANOVA with Tukeys multiple comparison test, where ***P<0.001, **P<0.01 compared to the positive control group.

111x62mm (150 x 150 DPI)

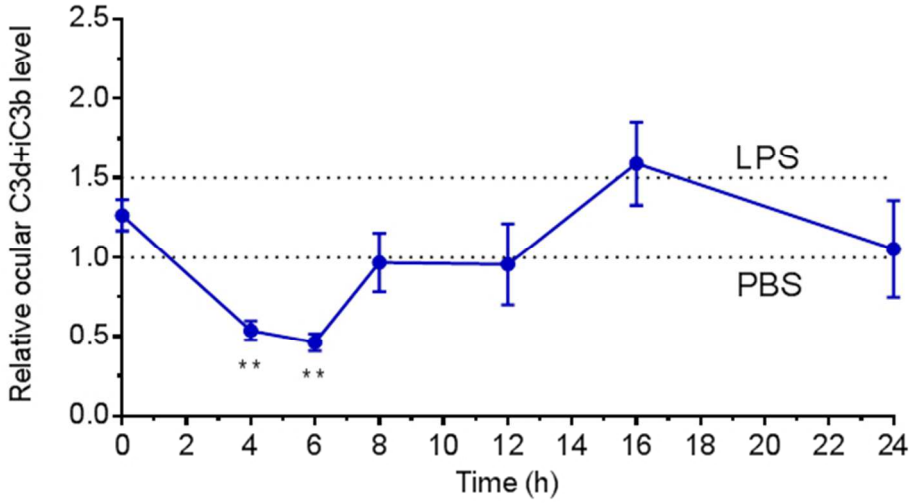

Figure 6/6B: same legend as 6A

111x62mm (150 x 150 DPI)

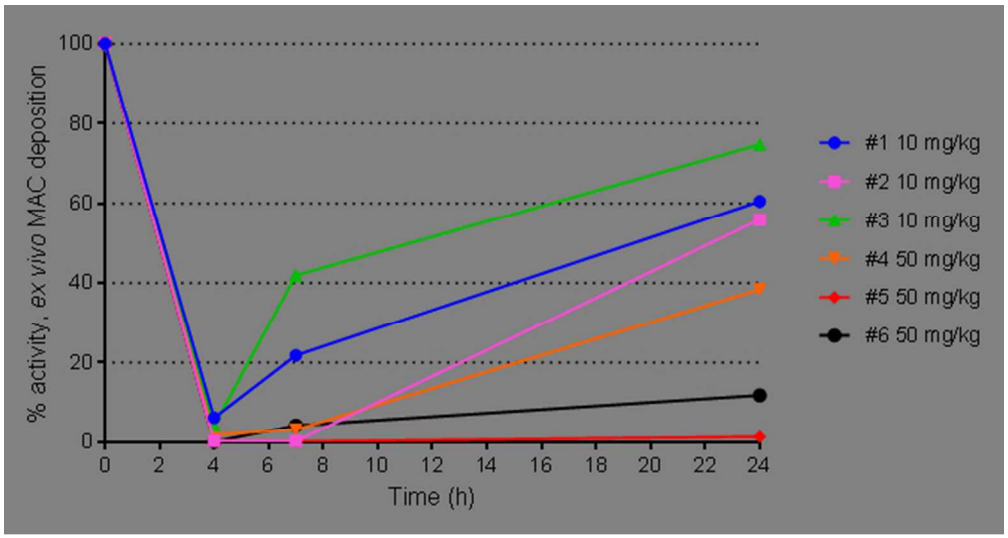

Figure 7: Inhibition of ex vivo MAC deposition after oral dosing of 2 to male cynomolgus monkeys. A single dose of 2 was administered by oral gavage at 10 mg/kg (n = 3) and 50 mg/kg (n = 3), respectively. Serum samples were obtained pre-dosing, and at 4, 7, and 24 hours after dosing, and complement activity was assessed with an ex vivo serum MAC deposition assay (A. The concentration of 2 in each sample relative to complement inhibition achieved was plotted in (B). The dotted lines indicate the 95% confidence band for the curve.

177x93mm (96 x 96 DPI)

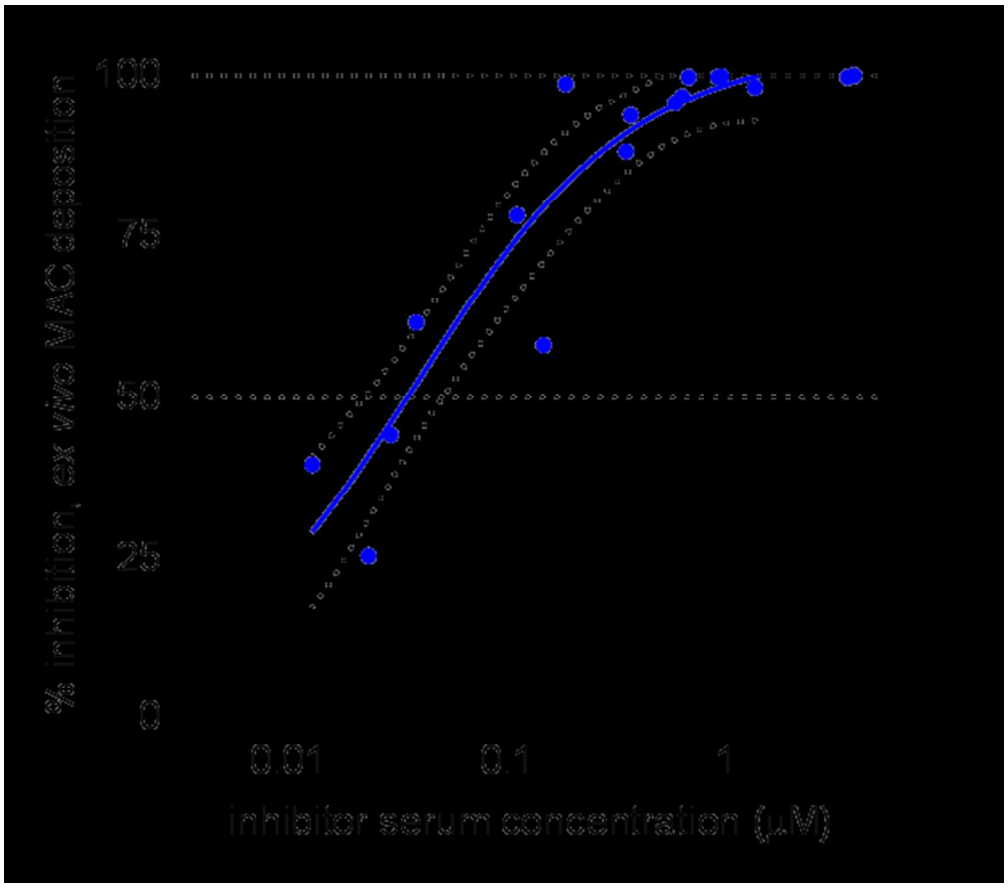

Same legend as for Figure 7.A.

105x92mm (150 x 150 DPI)

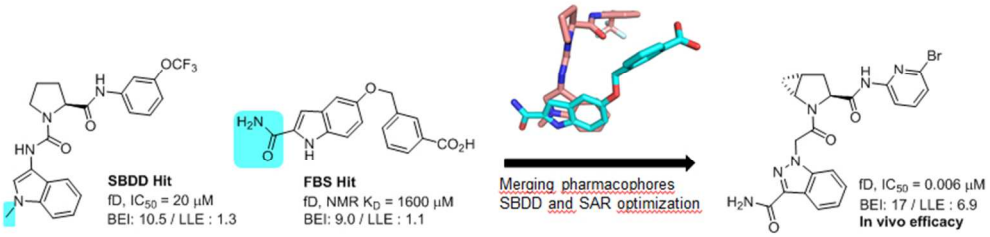

223x58mm (96 x 96 DPI)